Nature Communications

https://doi.org/10.1038/s41467-026-70004-2

Article in Press

Branched-chain α-keto acids impair glucose-stimulated insulin secretion in pancreatic β-cells under diabetes by reactivating the LDHA-lactate axis

Received: 11 April 2025

Accepted: 16 February 2026

Cite this article as: Lin, H., Ho, M.Y., Wang, B. *et al.* Branched-chain α-keto acids impair glucose-stimulated insulin secretion in pancreatic β-cells under diabetes by reactivating the LDHA-lactate axis. *Nat Commun* (2026). https://doi.org/10.1038/s41467-026-70004-2

Huige Lin, Melody Yuen Man Ho, Baomin Wang, Shama Mansoori, Yumei Yang, Wen Wang, Pui Kin So, Aimin Xu, Shilun Yang, Junlei Chang, Ada Man Hau Man, Hailong Piao, Chen Gao, Parco Ming Fai Siu, Xiaomu Li & Kenneth King Yip Cheng

Branched-chain α-keto acids impair glucose-stimulated insulin secretion in pancreatic β-cells under diabetes by reactivating the LDHA-lactate axis

Huige Lin[1], Melody Yuen Man Ho[1], Baomin Wang[1,2], Shama Mansoori[1], Yumei Yang[2], Wen Wang[3], Pui-Kin So[4], Aimin Xu[5,6,7], Shilun Yang[8], Junlei Chang[8], Ada Man Hau Man[1], Hailong Piao[3], Chen Gao[9], Parco Ming Fai Siu[10], Xiaomu Li[2,11*], Kenneth King Yip Cheng[1,12,13,14*]

Affiliations

[1] Department of Health Technology and Informatics, The Hong Kong Polytechnic University, Hong Kong, China

[2] Department of Endocrinology and Metabolism, Zhongshan Hospital Fudan University, Shanghai, China

[3] Dalian Institute of Chemical Physics, Chinese Academy of Sciences, Dalian, China

[4] University Research Facility in Life Sciences, Hong Kong Polytechnic University, Hong Kong, China

[5] The State Key Laboratory of Pharmaceutical Biotechnology, The University of Hong Kong, Hong Kong, China

[6] Guangdong–Hong Kong Joint Laboratory for Metabolic Medicine, The University of Hong Kong, Hong Kong, China

[7] Department of Medicine, The University of Hong Kong, Hong Kong, China

[8] Institute of Biomedicine and Biotechnology, Shenzhen Institute of Advanced Technology, Chinese Academy of Sciences, Shenzhen, China

[9] Departments of Pharmacology and Systems Physiology, University of Cincinnati, Cincinnati, USA

[10] School of Public Health, The University of Hong Kong, Hong Kong, China

[11] Department of Endocrinology and Metabolism, First Affiliated Hospital, College of Medicine, Zhejiang University, Hangzhou, China

[12] PolyU Shenzhen Research Institute, The Hong Kong Polytechnic University, China

[13] Research Institute for Future Food, The Hong Kong Polytechnic University, Hong Kong, China

[14] Research Centre for Chinese Medicine Innovation, The Hong Kong Polytechnic University, Hong Kong, China

*Correspondence: kenneth.ky.cheng@polyu.edu.hk and li.xiaomu@zs-hospital.sh.cn

Abstract

Dysmetabolism of branched-chain amino acid (BCAA) causes insulin resistance in type 2 diabetes, yet its effect on insulin-producing β-cells remains unclear. Here, we demonstrate that branched-chain α-ketoacids (BCKAs), derived from BCAAs, inhibited glucose-stimulated insulin secretion (GSIS) and glucose fluxes across human islets, mouse islets, and mouse β-cells. In diabetic humans, elevated circulating BCKAs negatively correlated with insulin secretory ability. Treatment with BCKA or its impaired catabolism suppressed GSIS in human islets and male mice, while reducing BCKA improved glucose tolerance and GSIS in male and female diabetic mice. Mechanistically, BCKA redirected glucose metabolism from the TCA cycle to the "β-cell disallowed" lactate dehydrogenase A (LDHA)-lactate axis. BCKA directly bound to LDHA, promoting its dimerization and enhancing enzymatic activity. β-cell-specific LDHA ablation restored GSIS and glucose tolerance in BCKA-fed male mice. Our findings demonstrate that BCKA disrupts insulin secretion through LDHA reactivation, linking aberrant BCAA metabolism to β-cell dysfunction in diabetes.

Introduction

Insulin secretion from pancreatic β-cells is tightly and dynamically regulated by multiple nutrients, hormones, and neural inputs. Glucose, the primary stimulator of biphasic insulin secretion[1], is taken up and metabolized via glycolysis to produce pyruvate, which enters the mitochondrial tricarboxylic acid (TCA) cycle to generate ATP. The resulting increase in ATP/ADP ratio closes the ATP-sensitive potassium (K_{ATP}) channel, inducing membrane depolarization and subsequent calcium influx, which drives a rapid but transient first-phase insulin secretion. Glucose also elicits a gradual but sustained second-phase insulin secretion through the K_{ATP} channel-independent amplifying signals and F-actin remodelling for exocytosis of insulin granules[2, 3]. This coupling of glucose metabolism to insulin secretion is essential for maintaining systemic glucose homeostasis.

Defective glucose-stimulated insulin secretion (GSIS) in β-cells is a major contributor to type 2 diabetes (T2D). Dysmetabolism of glucose through glycolysis and/or the mitochondrial TCA cycle impairs GSIS. For instance, disruption in pyruvate carboxylase-mediated anaplerotic flux of pyruvate to oxaloacetate, inhibition of pyruvate dehydrogenase-mediated pyruvate entry into the TCA cycle, or impaired TCA flux of α-ketoglutarate to isocitrate via isocitrate dehydrogenase 2 (IDH2), have all been shown to compromise GSIS[4, 5, 6, 7]. Additionally, altered expression or activity of glycolytic enzymes, such as lactate dehydrogenase A (LDHA; which converts pyruvate into lactate), glyceraldehyde 3-phosphate dehydrogenase (GAPDH) and phosphofructose-1-kinase (PFK1), also impairs GSIS[5, 8, 9].

Branched-chain amino acids (BCAAs), including leucine, isoleucine and valine, are essential amino acids. Beyond their role in protein synthesis, they also regulate energy metabolism and lipid handling in adipose tissues, as well as insulin sensitivity in the liver and skeletal muscle[10, 11, 12]. BCAAs are catabolized through transamination into α-ketoacids (BCKAs) via mitochondrial branched-chain aminotransferase (BCAT2), followed by decarboxylation via α-ketoacid dehydrogenase (BCKDH)

complex and further oxidation, yielding C3- and C5-acylcarnitines for lipogenesis and acetyl-CoA and succinyl-CoA as TCA cycle substrates. The BCKDH complex is positively and negatively controlled by protein phosphatase 1K (PPM1K) and branched-chain α-ketoacid dehydrogenase kinase (BDK) respectively, both targeting serine 293 of the E1α subunit (p-BCKDHA-Ser^{293})[13]. Under diabetic conditions, the activity and expression of these catabolic enzymes are altered in the insulin-responsive tissues[14, 15, 16], and enhancing BCAA catabolism improves insulin sensitivity in humans and rodents[10, 11, 17].

Interestingly, an *in vivo* isotope tracing study demonstrated that BCAAs are also catabolized in pancreas to supply approximately 20% of its TCA carbons, a rate much higher than in other tissues in rodents[18]. Although leucine and its direct catabolite α-ketoisocaproate (KIC) trigger β-cell acute insulin secretion[19, 20, 21], genetic alleles associated with high leucine levels correlate negatively with the homeostasis model assessment of β-cell function (HOMA-β) in diabetic patients[22]. Yet, whether β-cell BCAA metabolism is altered under the diabetic conditions and its contribution to β-cell dysfunction remain poorly understood.

In this study, we utilized various animal models and human samples to demonstrate that disrupted BCAA catabolism in diabetic β-cells drives accumulation of BCKAs, which act as protein linkers to induce dimerization of LDHA, a conventional "disallowed protein" in β-cells[23]. This LDHA activation redirects glucose metabolism from the TCA cycle to lactate production, reducing ATP production and ultimately impairing GSIS and glucose tolerance. While role of BCAA in insulin-responsive tissues is well recognized, our study demonstrated a novel mechanism linking BCAA dysmetabolism to β-cell dysfunction in T2D, highlighting the therapeutic potential of targeting β-cell metabolic dysregulation to restore glucose homeostasis in diabetes.

Results

Aberrant BCAA catabolism in diabetic islets and β-cells

It remains unknown whether BCAA catabolic machinery and their associated metabolites are altered and contribute to pancreatic β-cell dysfunctions in diabetes. Immunohistochemical staining revealed that total BCKDH-A, PPM1K, and BDK were abundantly expressed in the pancreatic islets of 20-week-old male BKS (*db/+*) lean mice, whereas BCAT2 was expressed similarly in both islets and exocrine cells. Notably, the expression of these proteins was significantly reduced in the pancreatic islets of BKS (*db/db*) diabetic mice (Fig. 1a-b), which displayed severe obesity, hyperglycemia, reduced insulin secretion, high serum levels of BCAAs and their downstream catabolites BCKAs, including [α-ketoisocaproate (KIC), α-keto-β-methylvalerate (KMV), and α-ketoisovalerate (KIV)] (Supplementary Fig. 1). Despite comparable phosphorylation levels of BCKDH-A—the key enzyme for BCAA catabolism, the p-BCKDH-A/total BCKDH-A ratio was markedly elevated in diabetic islets, suggesting reduced enzymatic activity and impaired BCAA metabolism (Fig. 1a-b). Ratio of p-BCKDH-A/total BCKDH-A was calculated individually for each mouse, rather than being normalized across the entire group, ensuring a more precise and individualized assessment. BCAAs and their metabolites were detected in isolated islets from the lean mice but were significantly higher in those from the *db/db* mice (Fig. 1c), which might be due to increased uptake of BCAAs from the circulation and/or defective BCAA catabolism in the islets.

We re-analyzed transcriptome and proteome datasets of human islets from HumanIslets online portal.[24] There were no significant changes in mRNA expression of the enzymes (*BCAT2*, *BCKDH complex*, *PPM1K* and *BDK*) responsible for the first two BCAA catabolic processes between normal and T2D subjects (Fig. 1d). By contrast, protein expressions of BCAT2, BCKDH-A, DLD and PPM1K were significantly diminished in islets of T2D subjects compared with those in non-T2D subjects (Fig. 1d). Notably, a previous study of gene co-expression and protein-protein interaction networks highlighted *PPM1K* as a prominent T2D candidate gene in human islets,[25] but its physiological relevance is

unexplored. To confirm that PPM1K expression is reduced in pancreatic β-cells, we performed co-immunofluorescence staining with insulin (as a β-cell marker) using the pancreatic sections from human donors with or without T2D (Supplementary Table 1). PPM1K was abundantly expressed in β-cells in non-diabetic (ND) human subjects, but its expression was markedly reduced in T2D subjects (Fig. 1e, g). Aligned with the change in PPM1K, phosphorylation of BCKDH-A-Ser^{293} (p-BCKDH-A-Ser^{293}) was increased in β-cells of diabetic subjects (Fig. 1f, g), while total BCKDH-A expression remained unchanged. The increased pBCKDH-A/total BCKDH-A ratio, along with reduced PPM1K expression in pancreatic β-cells were consistent with observations from *db/db* mice (Fig. 1a, b).

Circulating levels of BCKA negatively associate with β-cell function

Although circulating levels of BCAA and BCKA are known to be positively associated with peripheral insulin resistance in humans[26, 27], their association with β-cell function is unclear. In line with previous reports, we found that hyperglycemic individuals exhibited significantly higher circulating levels of BCAA and BCKA, along with a slight increase in C3- and C5-acylcarnitine levels (Supplementary Table 2). It is noteworthy that among these metabolites, only α-keto acids KIC and KMV displayed an inverse association with HOMA-β, an index for β-cell function (Supplementary Fig. 2a-h). Additionally, total circulating levels of BCKA negatively correlated fasting blood glucose (Supplementary Fig. 2i).

Next, we examined a direct relationship between insulin secretion and BCAA dysmetabolism in diabetic humans. We measured C-peptide levels during arginine stimulation test and fasting BCAA and their downstream metabolites in human diabetic patients. C-peptide but not insulin was used as an endogenous β-cell secretory index because this can avoid potential confounding effects from exogenous insulin treatment and the variability in hepatic insulin removal[28]. In T2D subjects, significantly negative associations between C3- and C5-acylcarnitines and arginine-stimulated C-peptide secretion (ArgIC%)

were observed, while such associations were not noted for BCAAs or BCKAs (Supplementary Fig. 3a-h). We then categorized the diabetic patients into two groups with a cutoff threshold response of C-peptide secretion at 2.1 ng/mL as previously reported[29]. The subjects with a level higher than 2.1 ng/mL were classified as "T2D with normal insulin secretion", while those with a level lower than 2.1 ng/mL were classified as "T2D with defective insulin secretion" (Supplementary Table 3). We found that C3- and C5-acylcarnitines remained significantly negatively associated with ArgIC% in both subgroups, while circulating leucine, valine, KIC, KMV and KIV were negatively correlated with ArgIC% only in the "T2D with defective insulin secretion" group (Supplementary Fig. 3i-o).

Excessive BCKA causes defective GSIS and glucose intolerance

We next examined the capacity of β-cells to utilize BCAA. Both MIN6 and INS-1E cells, the well-established insulinoma β-cell lines, express the BCAA catabolic machinery, including enzymes BCAT2, PPM1K, BDK and BCKDH-A. Acute treatment with mixtures of BCAAs or BCKAs reduced phosphorylation of BCKDH-A-Ser^{293}, accompanied with accumulation of BCAAs, BCKAs, and C3- and C5-acylcarnitines in β-cells and mouse islets (Supplementary Fig. 4).

Our findings from both humans and animal studies indicate that elevated circulating BCAA or their derived metabolites and/or aberrant β-cell BCAA metabolism may causatively induce β-cell dysfunction in T2D. To test the first possibility, we treated MIN6 β-cells with individual BCAA (leucine, isoleucine, valine), their corresponding BCKA (KIC, KMV, KIV), or acylcarnitines (C3- or C5-) at the concentrations matching their circulating levels in humans and mice with diabetes for 48 hours (Supplementary Fig. 5a-c). Only single BCKA at high concentrations (100 μM of KIC or KIV, or 200 μM of KMV) suppressed GSIS, (Supplementary Fig. 5b). We next evaluated whether combined exposure to BCAA or BCKA metabolites would exert a synergetic effect. A cocktail of BCAAs (leucine, isoleucine,

and valine, each at 0.8 mM) or BCKAs (KIC, KMV and KIV each at 10 μM; non-diabetic level) did not influence GSIS, whereas a BCKA cocktail (each at 30 or 100 μM, diabetic concentrations) significantly inhibited GSIS in mouse islets (Fig. 2a and Supplementary Fig. 5d). We replicated the inhibitory effect of BCKA cocktail (each at 30 μM) on GSIS in MIN6 β-cells and human islets (Fig. 2b, c). Importantly, treatment with 3,6-dichlorobenzo[b]thiophene-2-carboxylic acid (BT2)—a well-established inhibitor of BDK to facilitate BCKA catabolism[11, 30]—increased BCKDH-A activity and hence reduced BCKA accumulation in MIN6 cells and mouse pancreatic islets exposed to high BCKAs (Supplementary Fig. 6a-c), accompanied with restoration of GSIS (Fig. 2b). These results indicate that the concurrent elevation of all three BCKAs act synergistically to impair β-cell function. Of note, we used a BCKA cocktail containing KIC, KMV, and KIV (each at 30 μM) to treat the β-cells or islets in the subsequent experiments, unless otherwise specified.

We explored why chronic treatment with BCKA, but not BCAA, impairs GSIS, although BCAAs can also be catabolized into BCKAs. Chronic BCKA treatment for 48 hours dramatically increased intracellular KIC, KMV and KIV by 10-30-fold, without significantly affecting BCAA levels in both MIN6 and INS-1E β-cells (Supplementary Fig. 7). By contrast, BCAA treatment only modestly increased intracellular BCKA levels (Supplementary Fig. 7d-f, j-l). These data indicate that conversion the majority of BCAAs is not used for catabolism in pancreatic β-cells, at least, under normal culture conditions.

We next examined the second possibility of whether blocking β-cell BCKA catabolism impairs GSIS. siRNA-mediated *Bckdha* or *Ppm1k* silencing impaired GSIS in INS-1E β-cells, and such impairments were rescued in BCAA-free medium (Fig. 2d-g and Supplementary Fig. 6d-e). Likewise, pancreatic islets from PPM1K global knockout mice displayed a marked reduction of GSIS compared with those from their WT littermates (Fig. 2h). On the other hand, *Bcat2* silencing had no impact on GSIS (Supplementary Fig. 6f, g), which is similar to the observation in BCAT2 knockout mouse model[31].

Chronic BCKA supplementation causes defective GSIS and glucose intolerance in mice

We then investigated whether manipulation of circulating BCKA affects β-cell functions using two different animal models. In the first model, C57BL/6J mice received either BCKA mixture (KIC, KMV and KIV each at 5 mg/ml) or saline (vehicle control) via drinking water for 6 weeks. Circulating BCKA gradually increased in the BCKA-fed mice to approximately 75 μM, a level comparable to those observed in *db/db* diabetic mice or T2D subjects (Fig. 3a)[17]. BCKA administration had no obvious impact on circulating BCAA levels, food intake, body weight, short-term fasting blood glucose and insulin level as well as insulin sensitivity (Supplementary Table 4 and Fig. 3b), but induced progressive glucose intolerance and defective GSIS (Fig. 3c-f). On the other hand, arginine-induced insulin secretion was comparable between BCKA-fed and control mice (Fig. 3g). BCKA feeding upregulated protein expressions of BCKDH-A, PPM1K, and BDK in pancreatic islets, suggesting active transport of dietary BCKA into islets and induction of their catabolic machinery (Supplementary Fig. 8a). Meanwhile, BCKA feeding did not alter insulin content, islet size, or α-/ β-cell distribution (Supplementary Fig. 8b-e). These data suggest that BCKA induces glucose intolerance mainly by disrupting GSIS.

In the second animal model, we tested whether reducing circulating BCAA/BCKA levels improves β-cell function in *db/db* diabetic mice. After a week of BT2 treatment, circulating BCAAs and BCKAs levels were reduced by approximately 30-40% and 50-60%, respectively (Supplementary Fig. 9a, b, Supplementary Table 5). BT2 treatment alleviated glucose intolerance and improved GSIS (Supplementary Fig. 9c, d), but had minimal effect on insulin sensitivity, arginine-induced insulin secretion (Supplementary Fig. 9e, f) or pancreatic islet size (Supplementary Fig. 9g). The improvement in GSIS might be due to reduced systemic BCKA and/or upregulated β-cell BCKA catabolism, as indicated by decreased BCKDH-A-Ser^{293} phosphorylation in the diabetic islets (Supplementary Fig. 9h).

To validate the latter speculation, we isolated islets from diabetic and lean mice and treated them with BT2 or vehicle for 4 hours, followed by BCKA supplementation. Diabetic islets accumulated more intracellular BCKA than control islets (Supplementary Fig. 10a-c). As expected, BT2 treatment reversed BCKA accumulation in diabetic islets and restored GSIS (Supplementary Fig. 10a-d). Taken together, our *in vivo* and *ex vivo* findings suggest that BT2 effectively improves GSIS by reducing circulating BCKA and/or directly promoting BCKA catabolism in β-cells.

β-cell specific blockage of BCKA catabolism induces glucose intolerance and defective GSIS in mice

To study β-cell-specific BCKA dysmetabolism, we generated β-cell specific PPM1K knockout mice (PPM1K β-KO mice) by crossing PPM1K$^{flox/flox}$ mice with Ins2-Cre/ERT mice (Supplementary Fig. 11a). We targeted PPM1K but not BDK or BCKDH complex for the below reasons: (1) SNPs and mRNA expression of *PPM1K* are closely associated with insulin secretion, HbA1c and HOMA-β in humans[22, 25, 32]; (2) we observed a dramatic reduction of PPM1K protein in the diabetic islets from rodents and humans (Fig. 1a, e); (3) we and others showed that *Ppm1k* silencing or deletion disrupted BCKA catabolism and impaired GSIS in β-cells[25] (Fig. 2g, h). *Ppm1k* mRNA was decreased by ~80% in pancreatic islets isolated from PPM1K β-KO mice compared to WT controls (Fig. 4a), accompanied by a sharp increase in BCKA levels in the PPM1K-deficient islets (Fig. 4b). On the other hand, *Ppm1k* mRNA expression in skeletal muscle, subcutaneous white adipose tissue (sWAT) and liver as well as circulating BCAAs, KIC and KMV remained unchanged, while circulating KIV was modestly increased in the PPM1K β-KO mice (Supplementary Fig. 11b-d).

We and others have demonstrated that Ins2-Cre and Ins2-Cre/ERT mice have normal glucose tolerance and GSIS, therefore we only included PPM1K$^{flox/flox}$ littermates as WT controls[3, 33, 34, 35, 36]. PPM1K β-KO mice exhibited delayed glucose clearance and lower insulin secretion during GTT (Fig. 4c, d), but normal

insulin sensitivity and arginine-induced insulin secretion (Fig. 4e, f). β-cell-specific PPM1K deletion did not significantly affect islet size or β-/α-cell proportions (Supplementary Fig. 12). These findings suggest that selectively abrogating β-cell BCKA catabolism via PPM1K deletion induces defective GSIS and glucose intolerance in mouse model.

BCKA disrupts glucose metabolism in β-cells

In the subsequent mechanistic investigation, we mainly employed BCKA treatment or PPM1K inhibition to mimic β-cell BCKA dysmetabolism, unless otherwise specified. Consistent with the animal studies, *ex vivo* study of isolated pancreatic islets showed that BCKA treatment or β-cell-selective PPM1K deletion only abolished insulin secretion induced by glucose, but not potassium chloride (KCl; which directly induces insulin secretion via membrane depolarization) (Fig. 3h and 4g). Furthermore, dynamic insulin secretion assay showed that only first- but not second-phase GSIS was blocked by BCKA treatment or β-cell PPM1K deletion (Fig. 3i and 4h). GSIS involves a cascade of events starting with glucose uptake, followed by glycolysis and mitochondrial TCA cycle (Fig. 5a). To pinpoint the defective step in GSIS following chronic BCKA treatment, we assessed glucose uptake, ATP production, total intracellular insulin content, mitochondrial membrane potential, cell viability, caspase 3 activity and apoptotic gene expressions (Fig. 5b and Supplementary Fig. 13). Only glucose-stimulated ATP production was impaired (Fig. 5c), indicating a disruption in glucose metabolism.

Seahorse extracellular flux analysis was performed to monitor glucose metabolism, revealing that chronic BCKA treatment significantly reduced both glucose-stimulated extracellular acidification rate (ECAR; normally indicative for glycolytic flux) and oxygen consumption rate (OCR; reflecting mitochondrial respiration) (Fig. 5d, e). Notably, the interpretation of these results in β-cells is complicated by their unique metabolic characteristics. Unlike most other cell types, β-cells express minimal levels of

monocarboxylate transporter 1 (MCT; mediates lactate efflux), and lactate dehydrogenase A (LDHA) under normal conditions[37, 38, 39, 40]. Indeed, the near absence of MCT1 in normal β-cells makes it unlikely that the observed ECAR changes resulted from lactate-coupled proton efflux in anaerobic glycolysis, as typically assumed in conventional interpretations. Second, both our findings and previous reports showed that oligomycin (mitochondrial ATP synthase inhibitor) reduces ECAR in different β-cells and islets[33, 41, 42, 43, 44, 45], suggesting that a substantial portion of ECAR originates from mitochondrial CO_2-dependent acidification rather than anaerobic glycolysis. Therefore, the ECAR reduction in BCKA-treated β-cells likely reflected diminished respiratory CO_2 from mitochondrial oxidation, typically in β-cell models as previously reported[46]. The inhibitory effect of BCKA on ECAR and OCR were also reproduced in EndoC-βH1 cells, a well-characterized human β-cell line that closely mimics primary β-cells in GSIS (Supplementary Fig. 14)[47]. Furthermore, concomitant treatment with BT2 reversed the effects of BCKA on glucose-stimulated ECAR and OCR (Fig. 5d, e). Importantly, similar defects in glucose-stimulated ATP production, ECAR and OCR responses were observed in *Ppm1k*-silenced INS-1E cells and β-cell-specific PPM1K-deficient islets, with unchanged glucose uptake (Supplementary Fig. 15).

Metabolomics analysis revealed that BCKA treatment had minimal effect on most glycolytic metabolites, including glucose-6-phosphate (G6P), fructose 6-phosphate (Fru-6-P), fructose-1,6-bisphosphate (FBP), 3-phosphoglycerate (3PG) and phosphoenolpyruvate (PEP) (Supplementary Fig. 16a, b). However, BCKA significantly reduced glucose-stimulated pyruvate and its direct catabolite acetyl-CoA but increased lactate in MIN6 cells (Supplementary Fig. 16b, c). TCA cycle intermediates such as alpha-ketoglutarate (α-KG) and succinate showed a trend of reduction in BCKA-treated β-cells (Supplementary Fig. 16c).

BCKA reconnects glucose metabolism to the inactivated LDHA-lactate axis

We next directly examined whether BCKA affects glucose flux using a stable isotope-labeled glucose tracer and metabolomics analysis. After BCKA treatment, mouse islets and MIN6 cells were incubated with low (2 mM) or high (20 mM) concentrations of $^{13}C_6$-labeled glucose for 30 minutes (mimicking GSIS). $^{13}C_6$-glucose-derived M+3 pyruvate enters TCA cycle via the anaplerotic action of pyruvate carboxylase (PC) to generate M+3 oxaloacetic acid (OAA) and M+3 citrate, or via pyruvate dehydrogenase (PDH) to generate M+2 citrate (Fig. 5f). High-glucose stimulation enhanced ^{13}C incorporation into glucose-derived TCA cycle intermediates (Supplementary Fig. 17c-f). BCKA treatment dramatically diminished $^{13}C_6$- glucose-stimulated productions of pyruvate and downstream TCA metabolites (citrate, α-KG, succinate and malate) but provoked ^{13}C incorporation into lactate in both mouse islets and MIN6 cells (Fig. 5g-l and Supplementary Fig. 17). Mass isotopomer distribution analysis revealed that BCKA reduced citrate production (M+3 and M+2) through both PC- and PDH-mediated pyruvate metabolism, thereby limiting pyruvate entry into the TCA cycle (Fig. 5i and Supplementary Fig. 17c). Importantly, the effects of BCKA on labeled glucose flux into lactate and TCA cycle were consistently observed in pancreatic islets from human donors (Supplementary Fig. 18).

Next, we validated whether the reduced pyruvate entry into the TCA cycle contributes to the suppressive effect of BCKA on GSIS. To this end, we used KCl and cell-permeable TCA metabolites, including pyruvate, α-KG and succinate, which bypass pyruvate metabolism and directly stimulate insulin secretion[48, 49, 50]. BCKA blocked insulin secretion induced by pyruvate but not by succinate, α-KG or KCl, further supporting an impaired pyruvate metabolism in BCKA-treated β-cells (Supplementary Fig. 19a). To test whether promoting pyruvate entry into the TCA cycle reversed BCKA-induced GSIS defect, we inhibited PDH kinase using dichloroacetate (DCA), an activator of PDH that enhances pyruvate flux[51, 52.] DCA reduced PDHα1 phosphorylation, restored pyruvate entry into the TCA cycle, and largely reversed BCKA-induced GSIS defect (Supplementary Fig. 19b-i). These findings suggest that BCKA restricts pyruvate entry into the TCA cycle, leading to reduced production of ATP and other coupling factors for

insulin secretion.

Inhibition of PC or PDH impairs GSIS by impeding pyruvate entry to the TCA cycle[33, 53, 54], whereas LDHA overexpression blocks GSIS by disrupting mitochondrial function via an unknown mechanism[9, 55]. LDHA expression is suppressed in pancreatic β-cells[38, 39, 40], preventing pyruvate-to-lactate conversion to maximize the insulinotropic function of glucose. In BCKA-treated β-cells, the reduced pyruvate flux into TCA cycle could result from (1) impaired PC and/or PDH function, (2) LDHA activation or (3) both. BCKA treatment did not change expression of PC, PDH, phosphorylated PDH at serine 293, *Hif1α* (Hypoxia-inducible factor 1-alpha; a transcription factor for glycolytic pathway) or LDHA in β-cells (LDHA in Fig. 6a; PC, PDH and *Hif1α* in Supplementary Fig. 20a, b). However, *in vitro* enzymatic assays showed that BCKA upregulated LDHA activity in the isolated islets and MIN6 cells (Fig. 6b, c), whereas PDH and PC activities remained unchanged (Supplementary Fig. 20c, d). Likewise, BCKA raised the ratio of lactate to pyruvate stimulated by $^{13}C_6$-glucose in islets from human donors (Fig. 6d). BCKA also directly enhanced the enzymatic activity of purified human LDHA protein to produce lactate (Fig. 6e). Together, these results demonstrate that BCKA activates the "disallowed" LDHA-lactate axis in β-cells at a post-translational level.

β-cell LDHA deficiency restores glucose tolerance and GSIS in BCKA-fed mice

We next questioned whether LDHA inactivation could block the detrimental influences of BCKA on β-cells. Inhibition of LDHA by siRNA-mediated gene silencing or pharmacological inhibitor NHI-1 reversed BCKA-induced LDHA reactivation and defective GSIS (Supplementary Fig. 21a-e). Moreover, NHI-1 treatment directed glucose flux back to the TCA cycle in the BCKA-treated β-cells, as corroborated by increased ^{13}C incorporation into citrate, α-KG and OAA (Supplementary Fig. 21f-i).

To validate the role of LDHA in mediating BCKA effects *in vivo*, we generated tamoxifen-induced LDHA β-KO (*Ldha*$^{flox/flox}$ *Ins-Cre*$^{+ve}$) mice. Immunofluorescence staining confirmed a significantly reduced LDHA protein expression in pancreatic islets of LDHA β-KO mice compared to their WT littermates (Fig. 6f). β-cell specific LDHA deletion ameliorated the glucose intolerance and defective GSIS induced by BCKA feeding (Fig. 6g-j), while insulin sensitivity was not affected (Fig. 6k). To confirm these ameliorations are β-cell autonomous, we isolated pancreatic islets and consistently observed that BCKA diminished GSIS only in the islets from WT controls, but not those from LDHA β-KO mice (Fig. 6l).

Conversely, LDHA overexpression had opposite effects, increasing glucose-derived lactate while reducing citrate (Supplementary Fig. 22a-d), leading to impaired GSIS and ATP production in β-cells (Supplementary Fig. 22e-g). These effects were neutralized by BCAA deprivation (Supplementary Fig. 22b-f). Additionally, the inhibited GSIS by LDHA overexpression was counteracted by promoting pyruvate entry to the TCA cycle using DCA (Supplementary Fig. 22g).

Like the observations in the BCKA-treated β-cells, PPM1K or BCKDH-A inactivation enhanced LDHA enzymatic activity, and such increment was abolished by the LDHA inhibitor NHI-1 treatment (Supplementary Fig. 23a). The inhibitory effect of PPM1K and BCKDH-A inactivation or deletion on GSIS was abrogated by LDHA inactivation or PDH activation (Supplementary Fig. 23b-e). Glucose flux analysis showed that *Ppm1k* silencing upregulated ^{13}C-glucose-derived M+3 lactate and reduced M+2 citrate. Such defects were counteracted by PDH activator DCA (Supplementary Fig. 24a, b). Noticeably, DCA effectively enhanced ^{13}C-glucose incorporation into the TCA cycle metabolites, especially M+2 isotopologues, indicating restored glucose metabolism (Supplementary Fig. 24b-f). Unlike the observation in BCKA-treated β-cells, *Ppm1k* silencing did not affect M+3 isotopologues of citrate and OAA. The discrepancy might be due to the use of different β-cell lines and different intracellular BCKA

levels induced by PPM1K downregulation versus BCKA treatment. These data illustrate that intracellular BCKA dysmetabolism reconnects glucose flux to LDHA-lactate arm, reducing TCA cycle and mitochondrial coupling factor production, and hence impairing insulin secretion.

BCKA bridges LDHA monomer to enhance dimerization and enzymatic activity

A recent protein-metabolite interactomics study showed that LDHA binds multiple regulatory metabolites.[56] We hypothesized that BCKA can also bind to LDHA and activate its enzymatic function. To explore this, we performed Computational Molecular Docking Study using MOE (v2022.02) to predict the binding configuration of individual BCKA with LDHA. As shown in the 3D and 2D interaction diagrams (Fig. 7a and Supplementary Fig. 25 a), KIC and KMV bound at the interface of the LDHA dimer, forming a molecular bridge through hydrogen bonds with Ser210 on Chain A and Ser202 and Thr307 on Chain B. Similarly, KIV interacts with Gly203, Asn205, and Ser210 on Chain A, as well as Gly208 on Chain B. This binding configuration securely anchors each BCKA molecule within the binding pocket, as evidenced by the calculated binding free energy, which indicates a favorable interaction between the individual BCKA and the LDHA dimer. This bridging role of BCKA in linking Chain A and Chain B may potentially strengthen the association between the two chains, promoting LDHA dimerization or tetramerization and thereby enhancing its catalytic activity.

We validated the direct BCKA binding to purified human LDHA protein using Surface plasmon resonance (SPR) assays, giving dissociation constants (K_D) of 17.2 nM for KIC, 6.8 nM for KMV, and 3.6 nM for KIV, significantly lower than that of pyruvate (132 nM) (Fig. 7b). We further confirmed BCKA-LDHA interaction in β-cells using drug affinity-responsive target stability (DARTS) analysis[57.] This assay demonstrated that BCKA protected LDHA from proteinase K-induced degradation in a dose-dependent manner, comparable to the effect of pyruvate, the canonical binding substrate for LDHA

(Supplementary Fig. 25 b).

LDHA functions as a homotetrameric enzyme, with dimerization as an essential intermediate step for forming a tetramer[58]. Both tetrameric and dimeric forms of LDHA are more catalytically active than the monomeric form in converting pyruvate to lactate[59, 60, 61, 62]. We found in mouse islets, MIN6 and INS1-E β-cells, LDHA predominantly exists as monomers and dimers (Fig. 7c and Supplementary Fig. 26a-c). This might also explain LDHA inactivation in healthy β-cells. Treatment with BCKA increased dimeric LDHA in all three β-cell models, with tetramerization observed only in mouse islets (Fig. 7c and Supplementary Fig. 26a). To determine whether all three BCKAs are required for LDHA dimerization, we examined their effects individually and in combination. At 30 μM, no single BCKA induced LDHA dimerization, whereas combinations of two or three BCKAs effectively promoted dimer formation (Supplementary Fig. 26a). However, consistent to our GSIS results, higher concentration of individual BCKA, e.g., 100 μM KIC, 200 μM KMV or 100μM KIV, was able to enhance LDHA dimerization (Supplementary Fig. 26b). Additionally, DCA treatment did not affect BCKA-induced LDHA dimerization, suggesting the effect was independent of PDH activity (Supplementary Fig. 26c). In addition, BCKA, but not BCAA, dose-dependently enhanced dimerization of recombinant human LDHA protein without promoting tetramerization (Fig. 7d, Supplementary Fig. 26d).

Together, these results demonstrate that BCKA enhances LDHA activity by stabilizing its dimeric form to redirect glucose flux toward lactate production and away from the TCA cycle, thereby impairing insulin secretion.

To experimentally validate the predicted binding sites in LDHA with BCKA, we generated plasmids expressing wild-type (WT) LDHA with Flag epitope and its mutants: 1MUT (Ser210 mutated to alanine [Ser210A]; conserved across all BCKAs), 3MUT (Ser202A/Ser210A/Thr307A; KIC and KMV binding sites), and 4MUT (Gly203A/Gly208A/Asn205A/Ser210A; KIV binding sites). The empty vector or the

LDHA plasmids were transfected into HEK293T cells, followed by DARTS assay. BCKA treatment prevented proteinase-induced degradation of WT-LDHA but not the three LDHA mutants (Fig. 7e). Consistently, BCKA treatment enhanced dimerization of WT LDHA but not the three LDHA mutants (Supplementary Fig. 26e). These results confirm that Ser210 is essential to mediate LDHA-BCKA interaction and dimer stabilization.

Discussion

Recent research has illustrated that BCAA dysmetabolism contributes to T2D through inducing peripheral insulin resistance[63, 64, 65]. Our study further reveals how BCKA dysmetabolism impacts insulin-producing pancreatic β-cells. Under normal conditions, BCKAs are catabolized in mitochondria via the BCKDH complex to generate CoA derivatives, which enter the TCA cycle. In diabetic β-cells, PPM1K downregulation resulted in increased BCAA-derived BCKA, which impairs β-cells by desensitizing their glucose metabolism and insulin secretion. Specifically, BCKAs (KIC, KMV and KIV) bind to LDHA, triggering its dimerization and activation. The activated LDHA diverts glucose metabolism from the TCA cycle towards lactate production, thereby compromising production of glucose-derived coupling factors essential for insulin secretion and causing subsequent glucose intolerance in diabetes (Fig. 8).

In pancreatic β-cells, glucose-derived pyruvate is utilized in the TCA cycle to drive oxidative phosphorylation and produce insulin coupling factors[66]. This process is partially facilitated by inactivation of LDHA and MCT1, both defined as "β-cell disallowed gene"[67]. Inhibition of pyruvate entry into the TCA cycle via blockage of PC or PDH also results in diminished GSIS[53, 68]. In our study, BCKA did not alter PDH and PC expression or activity, consistent with previous study showing that BCKA do not affect PDH activity[69]. However, LDHA, which is typically silenced in healthy β-cells, is induced or "de-repressed" by diabetogenic factors such as hyperglycemia and senescence[70, 71]. Acute LDHA overexpression impairs mitochondrial functions and insulin secretion in pancreatic β-cells[9, 55], yet its

impact on glucose flux to the TCA cycle remains undetermined. Our glucose flux experiment revealed that LDHA overexpression or BCKA-mediated activation reduces pyruvate entry into the TCA cycle while enhancing pyruvate-to-lactate conversion. These changes coincide with reduced ATP production and mitochondrial oxidation. We showed that LDHA inactivation almost entirely reverses the suppressive effects of BCKA on GSIS, mitochondrial oxidation, and glucose flux to the TCA cycle in BCKA-treated β-cells, suggesting these defects are mainly due to LDHA activation. Indeed, LDHA overexpression redirects glucose flux away from the TCA cycle towards lactate production in tumor cells[72]. Our study underscores the importance of proper glucose-pyruvate flux to the TCA cycle for GSIS and highlights how this flux is disrupted under diabetic conditions with BCKA elevation.

Acute stimulation with α-keto acids KMV and KIC but not KIV is known to increase insulin secretion in pancreatic β-cells[19, 31]. Genetic deletion of mitochondrial *Bcat2* abolishes KIC- or KMV-induced insulin secretion, suggesting transamination of BCKA is required for their insulinotropic action[31]. Contrary to the acute effect, we showed that chronic BCKA exposure or disrupted BCKA catabolism abrogated GSIS, whereas *Bcat2* silencing had no significant impact. BCKA increases LDHA activity, which might act as a compensatory mechanism for removing excessive BCKA in pancreatic β-cells, because LDHA has been demonstrated to metabolize BCKA *in vitro*[73]. Formal proof of the role of LDHA in BCKA catabolism will require measuring BCKA flux in LDHA-deficient β-cells.

Intracellular BCAA and BCKA levels are controlled by their extracellular uptake and intracellular catabolism. We showed that BCKAs are accumulated in diabetic islets, which are associated with PPM1K reduction and p-BCKDHA induction. However, it is currently unclear whether β-cell BCAA/BCKA transportation is altered under the diabetic condition. While SLC25A44 has been identified as the primary carrier for BCAAs into the mitochondrial matrix[74], evidence suggests it may not serve as a universal carrier for their keto acid derivatives. Specifically, studies have shown that overexpression of SLC25A44

failed to promote the mitochondrial uptake of KIV[75]. Although MCT1 can mediate bidirectional BCKA transport across the plasma membrane[76] and is reported to also localize to mitochondrial membrane in most tissues[77], it is strictly disallowed within the β-cell plasma membrane to prevent inappropriate insulin secretion[37, 39]. Furthermore, neither MCT1 nor other MCT isoforms can be detected in islet β-cell mitochondria under normal physiological conditions[67]. Consequently, a significant knowledge gap remains regarding how BCKAs generated within the matrix are exported to the cytoplasm to bind LDHA and activate its activity toward lactate production. Elucidating these mitochondrial BCKA transport mechanisms is critical to understanding their potential role in driving β-cell dysfunction during the pathogenesis of diabetes.

LDHA mRNA level in pancreatic β-cells is positively correlated with HbA1c in humans[78]. Transcriptomic and proteomic studies have consistently shown increased LDHA expression in β-cells or islets from individuals with T2D[24, 79]. However, few studies have explored LDHA activity in β-cells under diabetic conditions. Our study revealed that in normal β-cells, LDHA primarily exists in its inactive monomeric forms, effectively preventing activation. Under diabetic conditions, LDHA is upregulated when BCKA accumulates in pancreatic β-cells. It is noteworthy that both tetrameric and dimeric LDHA are catalytically active, while the monomeric form is inactive[59, 60, 61, 62]. We found BCKA increases dimeric form of LDHA while decreasing monomeric form in β-cells. Interestingly, individual BCKA interacts with LDHA at the interface between two monomers within a dimer, acting as a “protein linker” to enhance dimerization.-LDHA has been shown to bind with different classes of metabolites, including ketoacids, adenosine nucleotides, and free and acylated CoA[56]. These metabolites also regulate LDHA activity and glucose metabolism. Collectively, our findings identify BCKA (KIC, KMV and KIV) as a novel class of metabolite that interacts with LDHA and enhances its activity in pancreatic β-cells. Further investigation is warranted to determine whether this regulatory axis also occurs in other cell types, particularly in cancer cells, which frequently exhibit BCAA dysmetabolism and LDHA activation[13, 72].

Metabolite-protein interaction has been shown to control cellular response and metabolism. Our current study showed that BCKAs but not BCAAs directly bind to LDHA and hence enhance its enzymatic activity toward lactate production. In addition, our mutagenesis experiment identified Ser210 of LDHA as a critical residue for mediating the LDHA–BCKA interaction and dimer stabilization. Apart from LDHA-lactate axis, BCKAs have been shown to bind mitochondrial pyruvate carrier (MPC) and block pyruvate uptake in hepatocytes[80]. Although we did not directly examine the effect of BCKA on pyruvate uptake in mitochondria, its involvement in defective GSIS is likely negligible. Because inactivation of LDHA or inhibition of PDH kinase by DCA is sufficient to restore glucose flux to the TCA cycle and GSIS, arguing that pyruvate flux but not its uptake in mitochondria is impaired. However, a direct labeled pyruvate uptake assay is required to further clarify MPC involvement. In vascular cells, BCKAs inhibit prolyl hydroxylase domain (PHD)2 enzyme activity and activate HIF1α, thereby inducing LDHA expression and lactate production[81]. In contrast, our study identifies a distinct mechanism in which BCKAs activate LDHA through post-translational modification and dimerization without affecting its expression. Of note, BCKA treatment did not affect *Hif-1α* mRNA or LDHA protein expression in β-cells, thereby excluding the potential effect of BCKAs on the PHD2-HIFα-LDHA axis.

Elevated BCAA/BCKA levels have been observed in individuals with obesity, insulin resistance, or T2D, which is primarily due to malfunctional BCAA catabolic machinery within adipose tissue, skeletal muscle, and the liver[65, 82]. Pharmacological activation of BCAA catabolism using sodium phenylbutyrate (NaPB) or BT2 reduced BCAA and BCKA levels in both T2D humans and rodents[10, 11, 17], contributing to improved insulin sensitivity and glucose tolerance. However, these studies did not evaluate the impact of such treatments on β-cell function and insulin secretion. Our study found that BT2 treatment significantly reduced circulating BCAA/BCKA levels and improved glucose tolerance and GSIS, but not insulin sensitivity, in *db/db* diabetic mice. The reason for the unchanged insulin sensitivity in our study remains unknown, but it could be due to the use of different rodent models (*db/db* vs *ob/ob*, high-fat diet-

induced obese model, and Zucker fatty rats) and the initiation of BT2 treatment at various stages of obesity/diabetes[10, 11, 17]. We conclude that the reduction of BCKA, rather than BCAA, improves β-cell function, as chronic BCKA feeding worsens GSIS without affecting circulating BCAA levels.

It was reported that BCKA induces insulin resistance by inhibiting insulin receptor substrate 1 (IRS1) phosphorylation through mTORC1 activation in muscle cells *in vitro*[83]. However, a 6-week BCKA treatment did not induce insulin resistance but impaired GSIS under standard diet feeding condition in our study. This suggests that pancreatic β-cells may be more susceptible to BCKA-induced toxicity, or that peripheral tissues such as muscle and liver have a higher capacity to remove BCKA, preventing BCKA accumulation and its pro-insulin resistance effect under the standard chow feeding condition. Likewise, a recent study showed that promoting BCAA catabolism in skeletal muscle and/or liver had no effect on insulin sensitivity[84]. Collectively, our findings suggest that high BCKA levels mainly affect pancreatic β-cell functions, with minimal impact on insulin sensitivity.

Apart from T2D, aberrant BCAA/BCKA metabolism have also been reported in T1D. An inverse association between circulating BCAA and endogenous insulin secretion was observed in T1D patients[85]. Longitudinal metabolomics in children progressing to T1D also revealed early metabolic dysregulation preceding autoimmunity, characterized by elevated BCAA and reduced keto-leucine levels before seroconversion[86]. In addition, high levels of BCKA or PPM1K deficiency triggers apoptosis in multiple cell types[87, 88, 89]. Recent studies suggest that aberrant cell death receptor pathway via TMEM219 also contributes to β-cell destruction in T1D[90, 91]. In our animal studies, pancreatic β-cell mass was not altered by chronic treatment with BCKA, BT2 or β-cell specific PPM1K deletion. *In vitro*, BCKA treatment did not exert obvious effect on survival or apoptosis in β-cells. Therefore, the direct involvement of BCKA metabolism in T1D development appears unlikely. Nevertheless, further validation of the role of PPM1K

or BCKA metabolism on β-cell function and mass using appropriate T1D animal models (such as non-obese diabetic mice and streptozotocin treatment) is warranted.

Circulating BCKAs are consistently elevated in patients with obesity, insulin resistance, and T2D, yet their role in β-cell pathology has remained unclear. Our work provides direct mechanistic evidence that BCKAs are not only as BCAA byproducts but active drivers of β-cell dysfunction. Our findings are clinically relevant and important. First, our data suggest that BCKA concentrations could serve as biomarkers for detecting defective insulin secretion in β-cells. Second, our results support that dietary restriction of BCAAs or promoting BCKA catabolism might be a feasible approach for treatment and management of diabetes. Indeed, pharmacological inactivation of BDK using NaPB and hence promoting BCAA/BCKA catabolism has recently demonstrated to improve hyperglycaemia and insulin sensitivity in human with diabetes[17], despite no assessment on β-cell function. Consistently, a short-term low BCAA diet significantly improved insulin sensitivity and hence reduced insulin secretion as well improved mitochondrial efficiency in adipose tissues of humans with T2D[92]. Our findings further support the modulations of β-cell insulin secretion via targeting BCAA dysmetabolism, such as adjusting BCAA intake, enhancing BCKDH activity, or pharmacologically activating PPM1K. Together, our study indicates that the proper BCAA metabolism not only in peripheral tissues but also in β-cells is important for glucose homeostasis.

Limitation of the study

While our current study is comprehensive in terms of animal and cell models, multiple key findings were also replicated in human samples. These include the effect of BCKA on GSIS and glucose flux in human islets and Endoβ1 cells, the expression of BCKA catabolic enzymes in healthy and diabetic human pancreatic islets, direct effects of BCKA/BCAA on purified human LDHA protein, and the association of circulating BCKA with the β-cell function index. Further, the impacts of PPM1K inhibition on GSIS and

glucose metabolism via LDHA would be validated in human islets, when the samples are more accessible. Given that BCKA selectively impairs GSIS in our study, we recognize that the association of BCKA with GSIS in human subjects would provide more direct evidence than current correlations with arginine-induced C-peptide secretion and the HOMA-β index. However, such clinical data and samples are currently unavailable in our laboratory. This limitation could potentially be addressed in the future using a Mendelian randomization approach. Finally, although BCKA accumulation was observed in the diabetic islets, its metabolic flux between transamination and oxidation as well as metabolic fates (such as entry into TCA cycle or as substrate for lipogenesis) need to be further investigated by isotope-labeling experiments.

Methods

Isolation and collection of human pancreatic islets and sections

To obtain human islets, pancreatic specimens were collected from non-diabetic humans by the Department of Liver Surgery and Transplantation in Zhongshan Hospital, Fudan University. The human pancreatic tissues were immediately stored in cold University of Wisconsin (UW) solution until weighing and pancreatic duct perfusion with cold collagenase P (0.2 mg/mL, Roche, Cat# 11213865001) prepared in Hanks' Balanced Salt Solution (HBSS, Gibco™, Cat# 14025076). The perfused pancreas was further digested at 37°C for 20 minutes and subjected to gradient centrifugation using density gradient reagents histopaque 1119 (Sigma-Aldrich, Cat# 1119-1) and 1077 (Sigma-Aldrich, Cat# 1077-1) at 4°C, 339 g for 30 minutes. The purified human islets were collected between the 2nd and 3rd layers of the gradient and then picked manually under a microscope. The isolated islets with similar sizes were subjected to treatment with BCKA and assessments of GSIS (5 size-matched islets in each sample) and isotope glucose flux analysis (500 size-matched islets in each sample). The subjects were diagnosed with or without T2D

according to the ADA standards.[93] Participants were sex- and age-matched. Sex was determined by self-report (male or female). Written informed consent was obtained from the participants. All procedures were carried out in compliance with the Helsinki Declaration and approved by the Ethical Review Committee of Zhongshan Hospital, Fudan University (No. B2021-853R).

Human pancreatic sections from non-T2D and T2D cadaveric donors were procured from the Department of Hepatology of Zhongshan Hospital, Fudan University. The subjects were diagnosed with or without T2D according to the ADA standards[93]. Participants were sex- and age-matched. Sex was determined by self-report (male or female). The procedures were approved by the Ethical Review Committee of Zhongshan Hospital, Fudan University (No. B2021-853R).

Association analysis between BCAA metabolites and pancreatic β-cell function in humans

For the acute arginine-induced C-peptide (ArgIC) assay, 136 patients diagnosed with T2D according to the ADA standards [haemoglobin (HbA1c) over 6.5%] were recruited in the Department of Endocrinology and Metabolism, Zhongshan Hospital, Fudan University. Patients receiving treatment with insulin secretagogues, such as DPP4i and SGLT2i, or having severe hepatic dysfunction, renal dysfunction, malignant tumors, pregnancy, or mental disorders were excluded. Circulating biomarkers related to glucose metabolism (HbA1c, glucose, insulin and C-peptide) were measured during routine blood tests. ArgIC assay was performed on overnight-fasted patients. A baseline blood sample was collected before arginine injection (0 min). A clamp tube was connected with normal saline to ensure no liquid extravasation, followed by intravenous injection of 5 g of arginine hydrochloride (Shanghai Xinyi Jinzhu Pharmaceutical Co. Ltd., 20 mL per tube) for 30 seconds. After injection, blood samples were obtained at 2, 4 and 6 minutes for measurements of blood glucose, C-peptide and insulin. The response of C-peptide secretion was assessed as the level at first 4 minutes minus the basal level as previously reported[29]. Subjects with a secretory level higher than 2.1 ng/mL were grouped into “T2D with normal

insulin secretory ability", whereas those with a level lower than 2.1 ng/mL were grouped as "T2D with defective insulin secretory ability" (n=18 and 43, respectively). C-peptide level of each individual is represented as a percentage over its basal level before arginine stimulation and the incremental area under the curve (AUC) was calculated. Clinical and metabolic characteristics of T2D subjects are listed in Supplementary Table 3. All procedures were carried out in compliance with the Helsinki Declaration and approved by the Ethical Review Committee of Zhongshan Hospital, Fudan University (No. B2020-180R).

To assess the associations of circulating BCAA, BCKA and C3/C5-acylcarnitines with fasting blood glucose and HOMA-β (%), human plasma samples were collected from 68- to 74-year-old males and females in the Hong Kong community as we previously described[94]. Subjects were assigned to the groups of normoglycemia with fasting blood glucose at 4.3-5.2 mM (n=28) or hyperglycemia with fasting blood glucose ≥ 5.6 mM (n=25). Clinical and metabolic characteristics of human subjects are listed in Supplementary Table 2. Participants were sex- and age-matched. Sex was determined by self-report (male or female). The experiment was approved by Human Ethics Committee of the Hong Kong Polytechnic University (approval number: HSEARS20180924002).

Transcriptomes and proteomics analysis of human islets

To compare the mRNA and protein expression of genes involved in BCAAs metabolism in pancreatic islets from non-diabetic (ND) and T2D individuals, we utilized processed transcriptome and proteome datasets from *Kolic et al* (PMID 38959864)[24]. Briefly, pancreatic islets were isolated from cadaveric donors, achieving >95% purity, with T2D diagnosis confirmed via HbA1c levels or family declaration. For the transcriptome analysis, RNA was extracted from 50 islets per donor, with quality control requiring an RIN score >5. The dataset comprised samples from 82 ND and 8 T2D age-matched donors. For the proteome analysis, approximately 300 islets per donor were examined from 118 ND and 15 T2D age-matched donors.

Animal models

Ppm1k$^{flox/flox}$ mice (C57BL/6N) were generated by Nanjing Biomedical Research Institute of Nanjing University, China. Briefly, a targeting vector containing *homologous arms*, a *loxP* site inserted between exons 2 and 3 of the *Ppm1k* gene, and a *neomycin resistant cassette* followed by another *loxP* site inserted between exons 3 and 4 of the *Ppm1k* gene were electroporated into ES cells to generate the *Flox allele* termed *Ppm1k*$^{flox/flox}$ mice. The full generation report, including floxed site sequencing and genotyping strategy, can be provided upon reasonable request. *Ldha*$^{flox/flox}$ mice were well-established, and provided by Prof. Aimin Xu from the University of Hong Kong[95]. Tamoxifen-induced β-cell-specific *Ppm1k* and *Ldha* knockout mice were created by crossing *Ppm1k*$^{flox/flox}$ and *Ldha*$^{flox/flox}$ mice with *Ins2-Cre/ERT* mice, resulting in PPM1K β-KO (*Ppm1k*$^{flox/flox}$ *Ins-Cre*$^{+ve}$) and LDHA β-KO (*Ldha*$^{flox/flox}$ *Ins-Cre*$^{+ve}$) mice, respectively. We and others have demonstrated that Ins2-Cre and Ins2-Cre/ERT mice have normal glucose tolerance and GSIS[3, 33, 34, 35, 36], therefore only WT littermates *Ppm1k*$^{flox/flox}$ and *Ldha*$^{flox/flox}$ were used as controls in this study. To induce disruption of the *Ppm1k* and *Ldha* gene, 5-week-old male PPM1K β-KO, LDHA β-KO and their WT littermates were intraperitoneally injected with tamoxifen (MedChemExpress, Cat# HY-13757A) at a dose of 4 mg per mouse for 4 times over a 7-day period. Three weeks later, the induced knockout efficiency was confirmed by gene or protein expression of *Ppm1k* and *Ldha* in the islets. Generation of PPM1K global knockout mice was reported in our previous study[96].

For BCKA feeding study, 16-week-old male C57BL/6J mice were obtained from the Hong Kong Polytechnic University. The C57BL/6J mice, LDHA β-KO mice and their WT littermates were given free access to drinking water supplemented with NaCl as vehicle control or BCKA [5 mg/mL of KIC (Cayman Chemical, Cat# 21052), KMV (Sigma-Aldrich, Cat# K7125) and KIV (Sigma-Aldrich, Cat# 198994) each] for 6 weeks.

db/db diabetic mice and their lean littermates (*db/+*) were obtained from the Chinese University of

Hong Kong. BT2 (Santa Cruz Biotechnology, Cat# sc-276559) was freshly dissolved in DMSO at a concentration of 150 mM and further diluted into 5% DMSO with 0.1 M sodium bicarbonate, pH 9.0. 20-24-week-old *db/db* mice were randomly assigned into two groups and intraperitoneally injected with vehicle (5% DMSO in 0.1 M sodium bicarbonate) or BT2 at 20 mg/kg body weight 5-6 times per week for 4 weeks.

Sex- and age-matched animals were used in each experiment. Animal numbers are specified in the respective figure legends. All the mice were housed in the Centralized Animal Facilities of the Hong Kong Polytechnic University with a 12-hour light/dark cycle, humidity (60-70%), and temperature (23 ± 1 ℃) control. All mice had free access to a standard chow (24.7 kcal% protein, 13.2 kcal% fat, and 62.1 kcal% carbohydrates; Cat# 5053, PicoLab Rodent Diet 2.0) and water during the experiments. All animal experiments were approved by the Department of Health, HKSAR Government (Ordinance Cap. 340), and the Animal Subjects Ethics Sub-Committee of the Hong Kong Polytechnic University (22-23/333-HTI-R-GRF and 17-18/87-HTI-R-HMRF).

Glucose tolerance test (GTT), insulin tolerance test (ITT), glucose- and arginine-stimulated insulin secretion in mice

For the GTT, PPM1K β-KO, LDHA β-KO mice and the BCKA-fed mice were fasted for 6 hours before intraperitoneal injection with glucose (2 g/kg body weight). Blood glucose was measured every 15 or 20 minutes via tail vein with a glucose meter (Roche Accu-Chek, USA). *db/db* diabetic mice and their littermates were fasted for 16 hours, followed by intraperitoneal injection of glucose (1 g/kg body weight). Serum was collected from tail vein for measuring glucose levels using a glucose assay kit (Nanjing Jiancheng Bioengineering Institute, Cat# F006-1-1) following manufacturer's instructions.

For the ITT, mice were fasted for 6 hours before intraperitoneal injection with insulin (1.25 U/kg for *db/db* mice and 0.5 U/kg for the other mice; Sigma-Aldrich, Cat# 91077C). Blood glucose was measured

every 15 minutes via tail veil using a glucose meter.

For the GSIS, blood samples were collected during GTT at 0, 10 and 30 minutes via tail vein. For arginine-stimulated insulin secretion, mice were fasted overnight before intraperitoneal injection of arginine (1 g/kg body weight), followed by blood collection at 0, 4 and 10 minutes after injection. Serum was separated for measurement of insulin concentration using a mouse insulin ELISA kit (Mercodia, Cat# 10-1247-01) according to manufacturer's instructions.

Isolation of primary pancreatic islets from mice

Mice were fasted for 4 hours and anesthetized. The common bile duct was clamped off at the duodenum, and the pancreas was perfused with 3 mL of collagenase P (0.6 mg/mL, Roche, Cat# 11213865001) in Hanks' Balanced Salt Solution (HBSS, Gibco™, Cat# 14025076) via common bile duct. The pancreas was then separated and incubated with 5 mL of collagenase P at 37℃ for 20 minutes, followed by vigorous hand shaking for 30 seconds and incubation at 37°C for an additional 5 minutes. The digestion process was halted by adding 15 mL of solution G (HBSS with 0.1% BSA). The digested pancreas was filtered with a 500-μm fine test sieve, and the filtrate was subsequently filtered again with a 70-μm cell strainer. Islets captured by the cell strainer were cultured in RPMI 1640 medium supplemented with 10% fetal bovine serum (FBS, Thermo Fisher Scientific, Cat# 10270), 1% penicillin-streptomycin (Thermo Fisher Scientific, Cat# 15140122) and 50 μM beta-mercaptoethanol (Bio-Rad Laboratories, Cat# 1610710) overnight at 37°C in an incubator with humidified atmosphere and 5% CO_2. The islets were manually picked under a microscope for insulin secretion assay or LC-MS/MS targeted metabolomic study.

Cell culture, transfection, and insulin secretion assay

The rat insulinoma cell line INS-1E (AddexBio Technologies, Cat# C0018009) and the mouse pancreatic β-cell line MIN6 (AddexBio Technologies, Cat# C0018008) were cultured in RPMI 1640 (Gibco, Cat#

31800105) or DMEM (Gibco, Cat# 12800082) supplemented with 15% FBS, 1% penicillin-streptomycin and 50 μM beta-mercaptoethanol. Human EndoC-βH1 cells (Human Cell Design)[47] were cultured in OPTIβ1® medium (Human Cell Design) according to manufacturer's instructions. 293T cells (Procell, Cat# CM-0005) were cultured in DMEM (Gibco, Cat# 12800082) supplemented with 10% FBS, 1% penicillin-streptomycin. The cells were cultured at 37°C in a 5% CO_2 incubator. The β-cells or isolated islets were treated with different concentrations of L-leucine (Sigma-Aldrich, Cat# L8000), L-isoleucine (Sigma-Aldrich, Cat# I2752), L-valine (Sigma-Aldrich, Cat# V0500), KIC, KMV, KIV, C2- (Sigma-Aldrich, Cat# A6706), C3-acylcarnitine (Sigma-Aldrich, Cat# 42602), C5-acylcarnitine (Sigma-Aldrich, Cat# 51371) or BT2 for 48 hours, or treated with NHI-1 (Merck Millipore, Cat# 533966) or sodium dichloroacetate (DCA; Tokyo Chemical Industry Co. Ltd., Cat# D1719) for 2 hours as indicated in each figure legend, followed by an insulin secretion assay. For the BCAA deprivation assay, the siRNA-transfected or adenovirus-infected β-cells were cultured in BCAA-free RPMI 1640 medium (USBiological Life Sciences, custom medium) for 24 hours. The control medium contained normal concentrations of BCAA by supplementing the BCAA-free medium with 0.381 mM of leucine, isoleucine and valine, respectively. INS-1E cells were transfected with either siRNA against *Ppm1k* (*siPpm1k*), *Bcat2 (siBcat2), Bckdha* (*siBckdha*), *Ldha* (*siLdha*) or *Scramble* controls (GenePharma) using Lipofectamine™ RNAiMAX reagent (Invitrogen, Cat# 13778150) for 48 hours according to the manufacturer's manual, or infected with adenovirus overexpressing human FLAG-tagged LDHA (WZ Biosciences Inc.) for 48 hours. The sequences of siRNA are listed in Supplementary Table 7. To validate the binding sites of BCKA on LDHA, pcDNA3.1 plasmids encoding LDHA WT, Ser210A (1MUT), Ser202A/Ser210A/Thr307A (3MUT), or Gly203A/Gly208A/Asn205A/Ser210A (4MUT) were constructed by YuYang Biosciences Inc. and further confirmed by DNA sequencing. These plasmids, along with empty vectors, were transfected into 293T cells using PEI (Polysciences, Cat# 23966-100) following the manufacturer's protocol. The transfected cells underwent binding analysis 48 hours post-

transfection or LDHA protein cross-linking assays after 48 hours of BCKA treatment.

For the insulin secretion assay, the cells or isolated islets were first cultured in Krebs buffer containing low glucose (2 mM) and 0.1% fatty acid-free BSA (Sigma-Aldrich, Cat# A8806) for 120 or 30 minutes, respectively. For static insulin secretion analysis, the cells were then stimulated for 30 minutes with low glucose (2 mM) as basal, high glucose (20 mM), KCl (40 mM), or cell-permeable form of methyl pyruvate (10 mM; Sigma-Aldrich, Cat# 371173), dimethyl α-ketoglutaric acid (α-KG; 30 mM; Sigma-Aldrich, Cat# 349631) or dimethyl succinate (30 mM; Sigma-Aldrich, Cat# 73605). For dynamic GSIS assay, conditional medium was collected every 3 minutes from the islets before and after stimulation with high glucose (20 mM). 0-9 min and 9-42 min were defined as the first- and second-phases of insulin secretion, respectively. Insulin concentration in the collected conditional medium was measured using an insulin ELISA kit (Antibody and Immunoassay Services, Cat# 32100) and normalized with protein concentration or islet size.

Targeted measurement of BCAA, BCKA and acylcarnitine by liquid chromatography-mass spectrometry (LC-MS)

Intracellular metabolites were measured by targeted metabolomics using the Agilent 6460 Liquid Chromatography-Electrospray Ionization Triple Quadrupole Mass Spectrometer (University Life Science, The Hong Kong Polytechnic University) connecting with different separating columns. For the measurements of BCAA-related catabolites, calibration curves were prepared using standard chemicals L-leucine, L-isoleucine, L-valine, KIC, KMV, KIV, C2-, C3- and C5-acylcarnitines. 10 μL of standard mixture, human plasma or mouse serum was extracted using 100 μL of chilled absolute methanol containing 0.5 μM D_8-valine (Cambridge Isotope Laboratories, Cat# DLM-311-PK) and 0.5 μM D_7-KIV (Cambridge Isotope Laboratories, Cat# DLM-4646-PK) as internal control standards. MIN6 or INS-1E β-cells were seeded onto 60-mm dishes. After the indicated experimental treatments, cells were washed

twice with cold PBS, extracted with 400 μL of cold 80% methanol containing internal standards and scraped into Eppendorf tubes. The metabolite extracts were vortexed or sonicated and centrifuged at 12,000 x g for 15 minutes under 4°C. To quantify BCAA and acylcarnitines, 2 μL of supernatant was injected into an Acquity UPLC BEH Amide Column (1.7 μm, 2.1×100 mm, Waters, Cat# 186004801) connected to the mass spectrometer. The target analytes were monitored by multiple reaction monitoring (MRM) in positive electrospray ionization (ESI) mode. The gradient mobile phase consisted of 5 mM ammonium formate (Sigma-Aldrich, Cat# 09735) and 0.1% formic acid (Sigma-Aldrich, Cat# 695076) in mobile phase A (water: acetonitrile, 90:10, v/v) and mobile phase B (water: acetonitrile, 10:90, v/v) at a flow rate of 0.3 mL/min.

Derivatization and measurement of BCKA were performed as previously described with some modifications[97]. Methanol-extracted cell samples were dried by the Refrigerated CentriVap Centrifugal Concentrator (Labconco) and then reconstituted with 40 μL of 80% methanol, followed by adding 500 μL of 12.5 mM o-phenylenediamine (OPD, Sigma-Aldrich, Cat# P9029) in 2 M HCl and incubation at 80°C for 20 minutes. The derivatized samples were cooled on ice and extracted with 500 μL of ethyl acetate containing 80 mg of Na_2SO_4. After centrifugation at 500 g for 5 minutes, the organic phase was transferred, and the aqueous phase was extracted again with 500 μL of ethyl acetate. The two organic phases were mixed with 80 mg of Na_2SO_4. After vortexing and centrifugation, the organic phase was dried and reconstituted with 200 mM ammonium acetate (Sigma-Aldrich, Cat# A1542). 2 μL of derivatized sample was injected into an Acquity UPLC BEH C18 Column, (130Å, 1.7 μm, 2.1 mm×50 mm, Waters, Cat# 186002350) for LC-MS analysis in positive ESI mode. The gradient mobile phase consisted of 0.1% formic acid in mobile phase A (water) and mobile phase B (acetonitrile) at a flow rate of 0.3 mL/min.

In all LC-MS analyses, the mass spectrometer was operated with the voltage set to 3.5 kV and the source temperature held at 300°C. The fragmentor voltage (70-110 V) and collision energy (5-25 psi) were also optimized for each metabolite. Blank controls were injected every 6 sample injections. The

number of samples in each group is specified in the respective figure legends. The target analytes were monitored by MRM with transition (precursor ion → product ion) determined for each metabolite as bellows: leucine (132.1→86.1), isoleucine (132.1→69.2), valine (118.1→72.2), KIC (203.2→161.2), KMV (203.2→174.2), KIV (189.1→119.3), C2-acylcarnitine (204.0→85.0), C3-acylcarnitine (218.0→85.0), C5-acylcarnitine (246.0→85.0), D8-valine (126.0→80.0), D7-KIV (196.0→120.0). The spectra were acquired by Agilent MassHunter Workstation Data Acquisition (VB.06.00) and were then analyzed using Agilent MassHunter Quantitative Analysis Software (V.B.06.00). Enrichment of each metabolite was quantified from calibration curves and corrected by internal control standards and protein concentration or islet size.

$^{13}C_6$-labeled glucose tracing study

Stocks of standard chemicals pyruvate (Sigma-Aldrich, Cat# P2256), lactate (BDH, Cat# 101384Q), citrate (Sigma-Aldrich, Cat# 251275), α-KG (Cayman Chemical, Cat# 33693), succinate (BDH, Cat# 102734W), malate (Sigma-Aldrich, Cat# 02288) and oxaloacetic acid (OAA; Cayman Chemical, Cat# 30280) were dissolved in water. Calibration curves were prepared by serial dilution of standard mixture in 80% methanol. MIN6 or INS-1E β-cells were seeded onto 100-mm dishes. After the indicated experimental treatments, MIN6 or INS-1E cells were subjected to serum and glucose starvation in Krebs buffer for 2 hours, while the isolated human and mouse islets were starved for 30 minutes. Subsequently, the cells or islets were stimulated with [U-$^{13}C_6$]-glucose (2 mM or 20 mM, or 10 mM for human islets; Cambridge Isotope Laboratories, Cat# CLM-1396-5) for 30 minutes. Next, the cells were harvested and extracted with chilled 80% methanol containing internal isotope standards. The metabolite extracts and standards were evaporated to dryness in a concentrator. Sample processing and metabolomic analysis were performed and MRM transition of TCA metabolites were acquired as previously described with minor modifications[98]. Briefly, the metabolite extract was reconstituted in 50 μL of water. Derivatization

was performed by adding 50 μL of 500 mM 1-ethyl-3-(3-dimethylaminopropyl) carbodiimide (EDAC; Sigma-Aldrich, Cat# 341006) and 100 μL of 250 mM *O*-benzylhydroxylamine hydrochloride (OBHA; Sigma-Aldrich, Cat# B22984) prepared in pyridine buffer (pH 5.0), followed by slow shaking at ambient temperature for 30 minutes. The derivatized metabolites were extracted twice using 400 μL of ethyl acetate and the organic phase was transferred for drying. The residues were resuspended in 30 μL of 50% methanol and injected into an Acquity UPLC BEH C18 column for LC-MS analysis in positive ESI mode. The gradient mobile phase consisted of 0.1% formic acid in mobile phase A (water) and mobile phase B (methanol) at a flow rate of 0.3 mL/min. The acquired spectra for isotopologues were quantified using Agilent MassHunter Quantitative Analysis Software. Signals of the labeled TCA cycle metabolites were corrected with parallel unlabeled control samples.

Targeted measurement of unlabeled glycolysis and TCA cycle metabolites

Following the specified experimental treatments, MIN6 cells were washed twice with cold PBS and flash-frozen in liquid nitrogen. Measurements of unlabeled glycolysis and TCA metabolites were performed by Hangzhou Lianchuan Biotechnology Co., Ltd. In addition, a second batch of samples was analyzed using capillary electrophoresis-mass spectrometry (CE-MS) with assistance from Prof. Hailong Piao at the Dalian Institute of Chemical Physics, Chinese Academy of Sciences[99]. Briefly, the treated cells were washed with 5% mannitol (Sigma-Aldrich, Cat# M4125), flash-frozen in liquid nitrogen, and extracted with 1 mL cold methanol containing 50 μM internal standards (methionine sulfone, Sigma-Aldrich, Cat# M0876; D-Campher-10-sulfonic acid sodium salt, Sigma-Aldrich, Cat# C2107). The samples were vortexed for 20 seconds, followed by adding 1 mL of chloroform and 400 μL of deionized water, with vortexing for 20 seconds after each addition. The mixtures were centrifuged at 14,000 g for 15 minutes at 4°C. The upper layer was filtered using an ultra-free MC centrifugal filter device (Millipore, Cat# UFC3LCC00) through centrifugation. The filtrate was evaporated to dryness using a concentrator, and

then dissolved in water containing Internal Standards 3 (Human Metabolome Technologies, Cat# H3304-1104, 1:200). The internal standard was used to standardize the metabolite intensity and adjust the migration time. The analysis of metabolites was performed using CE-QTOF MS (Agilent Technologies 7100A, connected with G6224A mass spectrometer). All samples were separated by the fused silica capillary [50 μm i.d. and total length of 80 cm; Human Metabolome Technologies (HMT)]. Data were processed and analyzed using Quantitative Analysis Software 10.2 (Agilent).

Intracellular lactate assay

Intracellular lactate was quantified by derivatization method and LC-MS as described above or a lactate assay kit (Sigma-Aldrich, Cat# MAK064) following the manufacturer's instructions. Briefly, cell lysates with 200 μg of protein were deproteinized with a 10 kDa MWCO spin filter (Millipore, Cat# UFC501096), and reacted with the reaction mixture and probe provided in the kit. Finally, absorbance was recorded at 570 nm by a microplate reader (Bio-rad Benchmark Plus MPM 5.1).

LDHA activity assay

LDHA enzymatic activity was analyzed following an online Worthington protocol (http://www.worthington-biochem.com/ldh/assay.html). Briefly, MIN6 and INS-1E β-cells were homogenized with 0.2 M Tris-HCl buffer (pH 7.3), sonicated and centrifuged. 20 μg of total protein from cell lysates was thoroughly mixed with pre-warmed reaction buffer to make final concentrations of 200 μM NADH (Cayman Chemical, Cat# 16078) and 1 mM sodium pyruvate (Sigma-Aldrich, Cat# P5280). Absorbance was immediately recorded at 340 nm per minute for 10 minutes using a microplate reader at 25°C. The LDHA activity was determined by a decrease in absorbance at 340 nm resulting from NADH oxidation (Bio-rad Benchmark Plus MPM 5.1).

.

PC activity assay

PC activity was measured using the PC activity kit (Solarbio, Cat# BC0735) according to manufacturer's instructions. Briefly, 5×10^6 cells were collected with 1 mL of extraction buffer. The cell lysates were treated with vehicle or 30 μM BCKA for 3 hours, and then mixed with reaction buffer. PC catalyzed pyruvate to oxaloacetic acid, which was then further converted to malate with an oxidation of NADH to NAD+. PC activity was determined by the rate of NADH oxidation, which was monitored by absorbance at 340 nm and normalized against protein concentration.

PDH activity assay

PDH activity was assessed using the PDH activity kit (Solarbio, Cat# BC0385) following manufacturer's instructions. In brief, 5×10^6 cells were lysed with extraction buffer. Cell lysates were treated with vehicle or 30 μM BCKA for 3 hours, and then mixed with reaction buffer. PDH catalyzed pyruvate to produce hydroxyethyl thiamine pyrophosphate, which further reduced 2,6-dichlorophenolindophenol to result in a decrease in absorbance at 605 nm. The change in absorbance was normalized against protein concentration.

Molecular docking analysis for metabolite-protein binding

3D molecular docking model and 2D diagram of the binding modes between human dimeric LDHA and KIC, KMV, and KIV were analyzed using Molecular Operating Environment (MOE) software 2022.02. The crystal protein structure of human LDHA was retrieved from the Protein Data Bank (PDB code: 8FW6). The parameters and subsequent minimization were consigned to the MMFF94x force field to optimize the molecular structure by minimizing the energy of the system. The prepared LDHA was defined as the receptor, and the binding site was defined by generating the α-site spheres in the site finder.

The docking BCKA (KIC, KMV, and KIV) attack the protein surfaces in their interior grooves for 30 trials until the most stable docking complexes are formed.

Drug affinity responsive target stability (DARTS)

To examine the binding between BCKA and LDHA protein, DARTS was performed as previously described with some modifications[100]. MIN6 β-cells were washed with PBS and solubilized in lysis buffer (0.2% Triton X-100, 200 mM NaCl, 50 mM Tris-HCl, pH 7.4; protease inhibitor cocktail After sonication and centrifugation, protein concentration was determined by BCA protein assay kit (Thermo Fisher Scientific, Cat# 23225). Cell lysates were diluted to the same protein concentration in chilled TNC reaction buffer (50 mM Tris-HCl, 50 mM NaCl, 10 mM CaCl2, pH 8.0), followed by incubation with different concentrations of BCKA and pyruvate for 1 hour on ice. After warming the reaction mixtures to room temperature, limited proteolysis was performed by adding 1 μg of proteinase K (Sigma-Aldrich, Cat# SAE0151) for every 700 μg protein and incubating at room temperature for 5 minutes. Digestion was then quenched by immediately adding SDS loading buffer and heating the mixture at 95°C for 5 minutes. The effect of BCKA or pyruvate to prevent proteolysis was analyzed by immunoblotting.

Surface plasmon resonance (SPR) assay

SPR assay was performed to investigate the interactions between individual BCKA (KIC, KMV and KIV), pyruvate and human recombinant LDHA protein (Abcam, Cat# AB93699) using a Sierra SPR®-32 Pro Analyzer with a high-capacity amine sensor chip (Bruker, Cat# 1862614) at room temperature. Protein immobilization was accomplished by an injection of 25 μg/mL LDHA protein in 10 mM sodium acetate (pH 5.5) and a running buffer containing 30 mM potassium phosphate, 150 mM NaCl, and 0.05% Tween 20 (pH 8.0). Immobilization levels typically reached 15,000 RU. BCKA were injected in a series of concentrations from 4.57 nM to 6.67 μM over the sensor chip with a running buffer containing 10 mM

Hepes, 200 mM NaCl, 1% DMSO, and 0.05% Tween 20 (pH 8.5). The binding kinetics (K_D) values were calculated based on the fitting curves using Sierra SPR control software R3.

Protein cross-linking assay

To examine the dimer and tetramer formation of LDHA in β-cells, a protein crosslinking assay was performed as previously described.[60] Isolated mouse pancreatic islets (470 islets/sample), MIN6 and INS-1E β-cells with or without chronic BCKA treatment were lysed by lysis buffer (40 mM HEPES, 150 mM NaCl, 0.1% NP-40, pH 7.5; protease inhibitor) and centrifuged. The protein crosslinking reaction was initiated by incubating cell lysates with 0.02% glutaraldehyde (Sigma-Aldrich, Cat# G6257) for 30 minutes in a 37°C water bath. The reaction was terminated by a final concentration of 50 mM glycine and SDS loading buffer. Protein samples were then analyzed by immunoblotting using LDHA, β-actin and HSP90 antibodies.

To examine the direct effect of BCKA and BCAA on dimerization and tetramerization of LDHA, 1 μg of human recombinant LDHA protein (Abcam, Cat# AB93699) was incubated with different concentrations of BCKA for 60 minutes on ice. Monomeric LDHA was obtained via heating at 99°C for 5 minutes. Different isoforms of LDHA were separated by SDS-PAGE and visualized by silver staining using a commercially available silver staining kit (Bio-rad, Cat# 1610449).

Immunoblotting analysis

Following the experimental treatments as specified in each figure legend, the cells were solubilized in a lysis buffer composed of 150 mM NaCl, 50 mM Tris-HCl (pH 7.4), 2 mM EDTA, 1% NP40 and proteinase inhibitor (MedChemExpress, Cat# HY-K0010). Protein samples were then resolved by SDS-PAGE and electro-transferred onto PVDF membranes. Proteins were subsequently analyzed with primary antibodies against BCAT2 (Abcam, Cat# ab95976), BCKDH-A (total and phospho-S293; Abcam, Cat#

ab90691 and Cat# ab200577), PPM1K (Proteintech, Cat# 14573-AP), HSP90 (Cell Signaling Technology, Cat# 4877), BCKDK (Sigma-Aldrich, Cat# HPA017995), β-actin (Santa Cruz, Cat# sc-8432), LDHA (Cell Signaling Technology, Cat# 2012) FLAG (Sigma-Aldrich, Cat# F7425), PC (Proteintech, Cat# 16588-1-AP), and PDHα1 (total and phosphor-S293; Cell Signaling Technology, Cat# 3205 and Cat# 37115). HSP90 or β-actin was used as a loading control. HRP-conjugated secondary antibodies, anti-rabbit (Cell Signaling Technology, Cat# 7074S) or anti-mouse (Cell Signaling Technology, Cat# 7076S) were used. EPSON Scan 3.10E was used to scan blots from X-ray films. Uncropped and unprocessed scans are provided in the Source Data file.

Histological, immunohistochemical (IHC) and immunofluorescence (IF) analyses

To calculate islet size, pancreas isolated from mice were fixed in 10% neutral buffered formalin, processed, embedded in paraffin, sectioned into 5-μm-thick slices, deparaffinized and rehydrated. the pancreatic sections were stained with hematoxylin for 10 minutes and eosin for 3 minutes (H&E staining), followed by dehydration with 100% ethanol twice, clearing in xylene for 10 minutes and mounting with DPX mounting medium. Images were captured using microscopy (BX35-DP80, Olympus) and analyzed using ImageJ V1.50 for quantification of islet area. A minimum of 5 parts of the pancreas and 2 tissue slides for each part were examined.

For IF, human or mouse pancreatic sections were heat retrieved at 98°C for 15 minutes in citrate buffer (10 mM sodium citrate, 0.05 % Tween 20, pH 6.0) and blocked in PBS with 3% BSA and 10% FBS at ambient temperature for 1 hour. The slides were co-stained with mouse anti-insulin (HyTest, Cat# 2IP10cc-D6C4cc) and rabbit anti- BCKDH-A (total and phospho-S293; Abcam, Cat# ab90691 and Cat# ab200577), PPM1K (Proteintech, Cat# 14573-1-AP) or glucagon (Sigma-Aldrich, Cat# SAB4501137) antibodies overnight at 4°C. The slides were then incubated with Alexa Fluor 594-anti rabbit IgG-(Invitrogen, Cat# A11012) and FITC-anti-mouse IgG-conjugated antibodies (Invitrogen, Cat# A11001)

for 90 minutes at ambient temperature in the dark. Finally, slides were mounted with Prolong glass antifade mountant containing DAPI (Invitrogen, Cat# P36984). The fluorescent images were captured using a Nikon Eclipse Ni-U Fluorescent Microscope and analyzed using ImageJ V1.50, normalized to islet size and analyzed consistently across samples. At least ten islets from different pancreatic regions were examined per human donor.

For IHC, mouse pancreatic sections were processed with antigen retrieval buffer and incubated with 3% hydrogen peroxide (H2O2) for 10 minutes at room temperature in the dark to quench endogenous peroxidases. After blocking, the slides were incubated overnight at 4°C with the primary antibodies against BCAT2 (Abcam, Cat# ab95976), BCKDH-A (total and phospho-S293), PPM1K, BCKDK (Sigma-Aldrich, Cat# HPA017995), LDHA (Cell Signaling Technology, Cat# 2012) or insulin. Following washing with PBST for three times, the slides were incubated with HRP-conjugated anti-rabbit (Cell Signaling Technology, Cat# 7074S) and anti-mouse (Cell Signaling Technology, Cat# 7076S) secondary antibodies for 90 minutes at room temperature. The chromogenic reaction was carried out with a DAB substrate kit (Abcam, Cat# ab64238) before counterstaining with hematoxylin and mounting. Images were acquired using a Nikon Y-THPL microscope and analyzed using ImageJ V1.50, normalized to islet size and analyzed consistently across samples. At least six islets from different regions of the pancreas were examined per mouse, using two levels of tissue sections per animal. Samples from two independent batches of mice were analyzed by two independent investigators.

Measurement of ATP production

MIN6 cells and INS-1E cells were seeded in a white 96-well plate with clear bottom and subjected to treatments as specified in each figure legend. Cells were starved in Krebs buffer supplemented with 2 mM glucose for 90 minutes, followed by stimulation with Krebs buffer supplemented with 2 mM or 20 mM glucose for 10 minutes. ATP level was measured using a luminescence ATP detection kit (PerkinElmer,

Cat# 6016943) according to manufacturer's instructions and the luminescence intensity was acquired using a Varioskan LUX Multimode Microplate Reader 7.0.2 (Thermo Fisher).

2-deoxy-D-glucose (2-DG) uptake assay

Glucose uptake was determined using the Glucose Uptake-Glo™ assay kit (Promega, Cat# J1341) according to the manufacturer's instructions. BCKA-treated MIN6 cells or siRNA-transfected INS1-E cells were subjected to glucose starvation for 2 hours, followed by incubation with a stable glucose analogue 2-Deoxy-d-glucose (2-DG; Cayman Chemical, Cat# 14325), which is transported across the membrane and rapidly phosphorylated in the same manner as glucose. The direct product of 2-DG, 2-deoxyglucose-6-phosphate (2DG6P), cannot be further metabolized by glycolysis and therefore reflects glucose uptake by cells. Stop buffer was added to lyse the cells and terminate the uptake of 2-DG. Intracellular production of 2DG6P was determined by sequential additions of neutralization buffer and 2DG6P detection reagent provided in the kit. Finally, luminescence intensity was recorded using a Varioskan LUX Multimode Microplate Reader (Thermo Fisher).

Measurement of mitochondrial membrane potential

Mitochondrial membrane potential was examined using TMRE mitochondrial membrane potential assay kit (Cayman Chemical, Cat# 701310). MIN6 cells were seeded in a black 96-well plate with clear bottom. Following treatment with BCKA for 48 hours, each well was added with 100 μL of 200 nM TMRE in 1 X assay buffer and incubated for 30 minutes at 37°C. The medium was subsequently removed, and the cells were gently rinsed twice with 1 X assay buffer. This was followed by addition of another 100 μL of 1 X assay buffer and the measurement of fluorescence intensity at excitation/emission 530/580 nm using a Varioskan LUX Multimode Microplate Reader (Thermo Fisher).

Assessment of extracellular acidification rate (ECAR) and oxygen consumption rate (OCR)

MIN6 cells and INS-1E cells were cultured in XF24 V7 PS tissue culture microplates (Agilent Technologies, Cat# 100777-004) at a confluence of 50-60%. The cells were subjected to treatment as specified in each figure legend. Prior to the analysis, XFe24 sensor cartridge (Agilent Technologies, Cat# 102340-100) was hydrated with Seahorse XF calibrant solution overnight at 37°C in a non-CO_2 incubator. The treated cells were washed twice and incubated with 500 μL of XF Base medium (pH 7.4; Agilent Technologies, Cat# 103335-100) for 1 hour in the non-CO_2 incubator. Following loading of the sensor cartridge and calibration of the Agilent Seahorse XFe24 analyzer, the cell culture plate was loaded into the analyzer. For the glycolysis stress test, ECAR and OCR were recorded during basal condition (2 mM glucose) and sequential injections of 20 mM glucose, 5 μM oligomycin (Cayman Chemical, Cat# 11341) and 50 μM 2-deoxy-D-glucose (2-DG; Cayman Chemical, Cat# 14325). The results were analyzed using Seahorse Wave Desktop 2.4.1 Software (Agilent Technologies) and normalized with protein concentration.

Real-time quantitative PCR analysis

Total RNA was isolated using the TRIzol reagent (Takara, Cat# 9109). cDNA was synthesized with 1 μg of RNA using the GoScript™ Reverse Transcription Kit (Promega, Cat #A2801). The real-time PCR reaction was conducted using the QuantiNova SYBR Green PCR Kit (Qiagen, Cat# 208056) and analyzed by the ViiA 7 Real-Time PCR System (Applied Biosystems). The mRNA expression level was analyzed using the ΔΔCt threshold cycle method and normalized against *β-actin*. The primers used were listed in Supplementary Table 6.

Cell viability assay

To assess cell viability, BCKA-treated β-cells were incubated with medium containing 0.25 mg/mL 3-

(4,5-dimethylthiazol-2-yl)-2,5-diphenyltetrazolium bromide (MTT; Solarbio Life Sciences, Cat# M1025) at 37°C in a CO_2 incubator for four hours. The culture medium was subsequently removed, and the purple crystal products formed by the cells were solubilized with 200 µL of DMSO, followed by shaking for 15 minutes and measurement of optical density at 570 nm.

Measurement of caspase-3 activity

Cell apoptosis was evaluated by quantifying caspase-3 enzymatic activity using the EnzChek Caspase-3 Assay Kit with the Z-DEVD-AMC substrate (Invitrogen, Cat# E13183). In brief, cells were rinsed with PBS, disrupted in the lysis buffer, and the resulting lysates were centrifuged at 5,000 x g for 5 minutes. An aliquot of lysate with 50 µg total protein was reacted with 2× substrate working solution for 30 minutes at room temperature, followed recording of fluorescent intensity at 342 nm excitation and 441 nm emission using a Thermo Scientific Varioskan LUX multimode reader. Caspase-3 activity was expressed relative to the protein content of each sample.

Statistical analysis

The data are expressed as mean ± standard error of mean (SEM). All statistical evaluations were conducted using Prism 10.1.2 (GraphPad Software). The sample size (n) of each experiment is specified in the figure legends. Prior to the application of parametric tests, all the data were pre-evaluated for normality and equal variance among the groups using D'Agostino-Pearson omnibus and Shapiro-Wilk normality test and Brown-Forsythe test, respectively. Statistical significance of normally distributed data with equal variance was evaluated using two-tailed Student's t-test for comparison between two groups, or one-way ANOVA with Tukey correction for multiple comparisons as indicated in the figure legends. The associations of circulating BCAA, BCKA, C3/C5 acylcarnitine with HOMA-beta, fasting blood glucose and arginine-induced C-peptide secretion were examined using Spearman correlation analysis. A

p-value <0.05 was deemed statistical significance. The representation of the p-value was *p<0.05, **p<0.01, or as specified in the figure legend. Animal experiments were conducted at least twice with each animal serving as a biologically independent sample. All cell experiments were replicated a minimum of three times.

Data availability

All experimental data generated in this study are provided in the Supplementary Information/Source Data file. A PDF file with uncropped scans of western blots and source data used to generate the graphs in the paper are provided. The processed transcriptome and proteome datasets for BCAA catabolic enzyme expression were downloaded from Kolic et al. (PMID: 38959864) and are publicly available at www.humanislets.com and were reanalyzed. Additional information can be obtained from the lead contact upon reasonable request.

References

1.Straub SG, Sharp GW. Glucose-stimulated signaling pathways in biphasic insulin secretion. *Diabetes Metab Res Rev* **18**, 451-463 (2002).

2.Campbell JE, Newgard CB. Mechanisms controlling pancreatic islet cell function in insulin secretion. *Nat Rev Mol Cell Biol* **22**, 142-158 (2021).

3.Wang B, *et al.* The adaptor protein APPL2 controls glucose-stimulated insulin secretion via F-actin remodeling in pancreatic beta-cells. *Proc Natl Acad Sci U S A* **117**, 28307-28315 (2020).

4.Hasan NM, *et al.* Impaired anaplerosis and insulin secretion in insulinoma cells caused by small interfering RNA-mediated suppression of pyruvate carboxylase. *J Biol Chem* **283**, 28048-28059 (2008).

5.Haythorne E, *et al.* Altered glycolysis triggers impaired mitochondrial metabolism and mTORC1 activation in diabetic beta-cells. *Nat Commun* **13**, 6754 (2022).

6.Lu D, *et al.* 13C NMR isotopomer analysis reveals a connection between pyruvate cycling and glucose-stimulated insulin secretion (GSIS). *Proc Natl Acad Sci U S A* **99**, 2708-2713 (2002).

7.Zhang GF, *et al.* Reductive TCA cycle metabolism fuels glutamine- and glucose-stimulated insulin secretion. *Cell Metab* **33**, 804-817 e805 (2021).
8.Ristow M, Vorgerd M, Mohlig M, Schatz H, Pfeiffer A. Deficiency of phosphofructo-1-kinase/muscle subtype in humans impairs insulin secretion and causes insulin resistance. *J Clin Invest* **100**, 2833-2841 (1997).
9.Ainscow EK, Zhao C, Rutter GA. Acute overexpression of lactate dehydrogenase-A perturbs beta-cell mitochondrial metabolism and insulin secretion. *Diabetes* **49**, 1149-1155 (2000).
10.Zhou M, *et al.* Targeting BCAA Catabolism to Treat Obesity-Associated Insulin Resistance. *Diabetes* **68**, 1730-1746 (2019).
11.White PJ, *et al.* The BCKDH Kinase and Phosphatase Integrate BCAA and Lipid Metabolism via Regulation of ATP-Citrate Lyase. *Cell Metab* **27**, 1281-1293.e1287 (2018).
12.Mansoori S, Ho MY, Ng KK, Cheng KK. Branched-chain amino acid metabolism: Pathophysiological mechanism and therapeutic intervention in metabolic diseases. *Obes Rev* **26**, e13856 (2025).
13.Sivanand S, Vander Heiden MG. Emerging Roles for Branched-Chain Amino Acid Metabolism in Cancer. *Cancer Cell* **37**, 147-156 (2020).
14.Lian K, *et al.* Impaired adiponectin signaling contributes to disturbed catabolism of branched-chain amino acids in diabetic mice. *Diabetes* **64**, 49-59 (2015).
15.Liu S, *et al.* Elevated branched-chain α-keto acids exacerbate macrophage oxidative stress and chronic inflammatory damage in type 2 diabetes mellitus. *Free Radic Biol Med* **175**, 141-154 (2021).
16.Yue SJ, *et al.* Berberine alleviates insulin resistance by reducing peripheral branched-chain amino acids. *Am J Physiol Endocrinol Metab* **316**, E73-e85 (2019).
17.Vanweert F, *et al.* A randomized placebo-controlled clinical trial for pharmacological activation of BCAA catabolism in patients with type 2 diabetes. *Nat Commun* **13**, 3508 (2022).
18.Neinast MD, *et al.* Quantitative Analysis of the Whole-Body Metabolic Fate of Branched-Chain Amino Acids. *Cell Metab* **29**, 417-429.e414 (2019).
19.Panten U, Christians J, von Kriegstein E, Poser W, Hasselblatt A. Studies on the mechanism of L-leucine-and alpha-ketoisocaproic acid-induced insulin release from perifused isolated pancreatic islets. *Diabetologia* **10**, 149-154 (1974).
20.Branstrom R, Efendic S, Berggren PO, Larsson O. Direct inhibition of the pancreatic beta-cell ATP-regulated potassium channel by alpha-ketoisocaproate. *J Biol Chem* **273**, 14113-14118 (1998).

21.Yang J, *et al.* Leucine Regulation of Glucokinase and ATP Synthase Sensitizes Glucose-Induced Insulin Secretion in Pancreatic β-Cells. *Diabetes* **55**, 193-201 (2006).
22.Lotta LA, *et al.* Genetic Predisposition to an Impaired Metabolism of the Branched-Chain Amino Acids and Risk of Type 2 Diabetes: A Mendelian Randomisation Analysis. *PLoS medicine* **13**, e1002179 (2016).
23.Sekine N, *et al.* Low lactate dehydrogenase and high mitochondrial glycerol phosphate dehydrogenase in pancreatic beta-cells. Potential role in nutrient sensing. *J Biol Chem* **269**, 4895-4902 (1994).
24.Kolic J, *et al.* Proteomic predictors of individualized nutrient-specific insulin secretion in health and disease. *Cell Metab* **36**, 1619-1633.e1615 (2024).
25.Taneera J, *et al.* A systems genetics approach identifies genes and pathways for type 2 diabetes in human islets. *Cell Metab* **16**, 122-134 (2012).
26.Vanweert F, Schrauwen P, Phielix E. Role of branched-chain amino acid metabolism in the pathogenesis of obesity and type 2 diabetes-related metabolic disturbances BCAA metabolism in type 2 diabetes. *Nutr Diabetes* **12**, 35 (2022).
27.Lynch CJ, Adams SH. Branched-chain amino acids in metabolic signalling and insulin resistance. *Nat Rev Endocrinol* **10**, 723-736 (2014).
28.Ratheiser K, Reitgruber W, Komjati M, Bratusch-Marrain P, Vierhapper H, Waldhäusl WK. Quantitative and qualitative differences in basal and glucose- and arginine-stimulated insulin secretion in healthy subjects and different stages of NIDDM. *Acta Diabetol Lat* **27**, 197-213 (1990).
29.Shen Y, *et al.* Association between 1,5-Anhydroglucitol and Acute C Peptide Response to Arginine among Patients with Type 2 Diabetes. *J Diabetes Res* **2020**, 4243053 (2020).
30.Tso SC, *et al.* Benzothiophene carboxylate derivatives as novel allosteric inhibitors of branched-chain alpha-ketoacid dehydrogenase kinase. *J Biol Chem* **289**, 20583-20593 (2014).
31.Zhou Y, Jetton TL, Goshorn S, Lynch CJ, She P. Transamination is required for alpha-ketoisocaproate but not leucine to stimulate insulin secretion. *J Biol Chem* **285**, 33718-33726 (2010).
32.Gheibi S, *et al.* Reduced Expression Level of Protein Phosphatase PPM1E Serves to Maintain Insulin Secretion in Type 2 Diabetes. *Diabetes* **72**, 455-466 (2023).
33.Li X, *et al.* The MDM2-p53-pyruvate carboxylase signalling axis couples mitochondrial metabolism to glucose-stimulated insulin secretion in pancreatic β-cells. *Nat Commun* **7**, 11740 (2016).
34.Yang Y, *et al.* The mitochondrial enzyme pyruvate carboxylase restricts pancreatic β-cell senescence by blocking p53 activation. *Proc Natl Acad Sci U S A* **121**, e2401218121 (2024).

35.Lee H, *et al.* Beta Cell Dedifferentiation Induced by IRE1α Deletion Prevents Type 1 Diabetes. *Cell Metab* **31**, 822-836.e825 (2020).
36.Lee H, *et al.* Stress-induced β cell early senescence confers protection against type 1 diabetes. *Cell Metab* **35**, 2200-2215.e2209 (2023).
37.Pullen TJ, Sylow L, Sun G, Halestrap AP, Richter EA, Rutter GA. Overexpression of monocarboxylate transporter-1 (SLC16A1) in mouse pancreatic β-cells leads to relative hyperinsulinism during exercise. *Diabetes* **61**, 1719-1725 (2012).
38.Sanchez PKM, *et al.* LDHA is enriched in human islet alpha cells and upregulated in type 2 diabetes. *Biochemical and biophysical research communications* **568**, 158-166 (2021).
39.Schuit F, *et al.* β-cell-specific gene repression: a mechanism to protect against inappropriate or maladjusted insulin secretion? *Diabetes* **61**, 969-975 (2012).
40.Rutter GA, Georgiadou E, Martinez-Sanchez A, Pullen TJ. Metabolic and functional specialisations of the pancreatic beta cell: gene disallowance, mitochondrial metabolism and intercellular connectivity. *Diabetologia* **63**, 1990-1998 (2020).
41.Montemurro C, *et al.* IAPP toxicity activates HIF1α/PFKFB3 signaling delaying β-cell loss at the expense of β-cell function. *Nat Commun* **10**, 2679 (2019).
42.Cornell D, *et al.* Pseudoislet Aggregation of Pancreatic β-Cells Improves Glucose Stimulated Insulin Secretion by Altering Glucose Metabolism and Increasing ATP Production. *Cells* **11**, (2022).
43.Hals I, *et al.* Time dynamics of elevated glucose and beta-hydroxybutyrate on beta cell mitochondrial metabolism. *Islets* **17**, 2503515 (2025).
44.Sentjens K, Pillai R, Joseph JW. The effects of free fatty acid-free bovine serum albumin and palmitate on pancreatic β-cell function. *Islets* **17**, 2479911 (2025).
45.Xiong X, *et al.* Sirtuin 6 regulates glucose-stimulated insulin secretion in mouse pancreatic beta cells. *Diabetologia* **59**, 151-160 (2016).
46.Mookerjee SA, Goncalves RLS, Gerencser AA, Nicholls DG, Brand MD. The contributions of respiration and glycolysis to extracellular acid production. *Biochim Biophys Acta* **1847**, 171-181 (2015).
47.Tsonkova VG, *et al.* The EndoC-βH1 cell line is a valid model of human beta cells and applicable for screenings to identify novel drug target candidates. *Mol Metab* **8**, 144-157 (2018).
48.Davis JC, *et al.* Glucose Response by Stem Cell-Derived β Cells In Vitro Is Inhibited by a Bottleneck in Glycolysis. *Cell Rep* **31**, 107623 (2020).

49.Rabaglia ME, Gray-Keller MP, Frey BL, Shortreed MR, Smith LM, Attie AD. Alpha-Ketoisocaproate-induced hypersecretion of insulin by islets from diabetes-susceptible mice. *Am J Physiol Endocrinol Metab* **289**, E218-224 (2005).
50.Ishihara H, Maechler P, Gjinovci A, Herrera PL, Wollheim CB. Islet beta-cell secretion determines glucagon release from neighbouring alpha-cells. *Nat Cell Biol* **5**, 330-335 (2003).
51.Stabenow LK, *et al.* Oxidative Glucose Metabolism Promotes Senescence in Vascular Endothelial Cells. *Cells* **11**, (2022).
52.Li Y, *et al.* Acetate supplementation restores chromatin accessibility and promotes tumor cell differentiation under hypoxia. *Cell Death Dis* **11**, 102 (2020).
53.Srinivasan M, *et al.* ß-Cell-specific pyruvate dehydrogenase deficiency impairs glucose-stimulated insulin secretion. *Am J Physiol Endocrinol Metab* **299**, E910-917 (2010).
54.Wang X, *et al.* Conditional knockout of pyruvate dehydrogenase in mouse pancreatic β-cells causes morphological and functional changes. *Mol Med Rep* **21**, 1717-1726 (2020).
55.Zhao C, Rutter GA. Overexpression of lactate dehydrogenase A attenuates glucose-induced insulin secretion in stable MIN-6 beta-cell lines. *FEBS Lett* **430**, 213-216 (1998).
56.Hicks KG, *et al.* Protein-metabolite interactomics of carbohydrate metabolism reveal regulation of lactate dehydrogenase. *Science* **379**, 996-1003 (2023).
57.Yang Y, Zhang Z, Li W, Si Y, Li L, Du W. αKG-driven RNA polymerase II transcription of cyclin D1 licenses malic enzyme 2 to promote cell-cycle progression. *Cell Rep* **42**, 112770 (2023).
58.Jafary F, Ganjalikhany MR, Moradi A, Hemati M, Jafari S. Novel Peptide Inhibitors for Lactate Dehydrogenase A (LDHA): A Survey to Inhibit LDHA Activity via Disruption of Protein-Protein Interaction. *Sci Rep* **9**, 4686 (2019).
59.Yamamoto S, Storey KB. Dissociation-association of lactate dehydrogenase isozymes: influences on the formation of tetramers versus dimers of M4-LDH and H4-LDH. *Int J Biochem* **20**, 1261-1265 (1988).
60.Liu Y, *et al.* Nuclear lactate dehydrogenase A senses ROS to produce α-hydroxybutyrate for HPV-induced cervical tumor growth. *Nat Commun* **9**, 4429 (2018).
61.Girg R, Rudolph R, Jaenicke R. The dimeric intermediate on the pathway of reconstitution of lactate dehydrogenase is enzymatically active. *FEBS Lett* **163**, 132-135 (1983).
62.Girg R, Jaenicke R, Rudolph R. Dimers of porcine skeletal muscle lactate dehydrogenase produced by limited proteolysis during reassociation are enzymatically active in the presence of stabilizing salt. *Biochem Int* **7**, 433-441 (1983).

63.Newgard CB, *et al.* A branched-chain amino acid-related metabolic signature that differentiates obese and lean humans and contributes to insulin resistance. *Cell Metab* **9**, 311-326 (2009).
64.Jang C, *et al.* A branched-chain amino acid metabolite drives vascular fatty acid transport and causes insulin resistance. *Nature medicine* **22**, 421-426 (2016).
65.Neinast M, Murashige D, Arany Z. Branched Chain Amino Acids. *Annu Rev Physiol* **81**, 139-164 (2019).
66.Prentki M, Matschinsky FM, Madiraju SR. Metabolic signaling in fuel-induced insulin secretion. *Cell Metab* **18**, 162-185 (2013).
67.Zhao C, Wilson MC, Schuit F, Halestrap AP, Rutter GA. Expression and distribution of lactate/monocarboxylate transporter isoforms in pancreatic islets and the exocrine pancreas. *Diabetes* **50**, 361-366 (2001).
68.Xu J, Han J, Long YS, Epstein PN, Liu YQ. The role of pyruvate carboxylase in insulin secretion and proliferation in rat pancreatic beta cells. *Diabetologia* **51**, 2022-2030 (2008).
69.Li T, *et al.* Defective Branched-Chain Amino Acid Catabolism Disrupts Glucose Metabolism and Sensitizes the Heart to Ischemia-Reperfusion Injury. *Cell Metab* **25**, 374-385 (2017).
70.Haythorne E, *et al.* Diabetes causes marked inhibition of mitochondrial metabolism in pancreatic β-cells. *Nat Commun* **10**, 2474 (2019).
71.Aguayo-Mazzucato C, *et al.* Acceleration of beta Cell Aging Determines Diabetes and Senolysis Improves Disease Outcomes. *Cell Metab* **30**, 129-142 e124 (2019).
72.Chen Y, *et al.* LDHA-mediated metabolic reprogramming promoted cardiomyocyte proliferation by alleviating ROS and inducing M2 macrophage polarization. *Redox Biol* **56**, 102446 (2022).
73.Heemskerk MM, van Harmelen VJ, van Dijk KW, van Klinken JB. Reanalysis of mGWAS results and in vitro validation show that lactate dehydrogenase interacts with branched-chain amino acid metabolism. *Eur J Hum Genet* **24**, 142-145 (2016).
74.Yoneshiro T, *et al.* BCAA catabolism in brown fat controls energy homeostasis through SLC25A44. *Nature* **572**, 614-619 (2019).
75.Walejko JM, *et al.* Branched-chain α-ketoacids are preferentially reaminated and activate protein synthesis in the heart. *Nat Commun* **12**, 1680 (2021).
76.Silva LS, *et al.* Branched-chain ketoacids secreted by glioblastoma cells via MCT1 modulate macrophage phenotype. *EMBO Rep* **18**, 2172-2185 (2017).
77.Chen L, *et al.* MCT1-mediated Lactate Shuttle to Mitochondria Governs Macrophage Polarization and Modulates Glucose Homeostasis by Affecting β Cells. *Adv Sci (Weinh)* **12**, e14760 (2025).

78.Malmgren S, *et al.* Tight coupling between glucose and mitochondrial metabolism in clonal beta-cells is required for robust insulin secretion. *J Biol Chem* **284**, 32395-32404 (2009).
79.Marselli L, *et al.* Gene expression profiles of Beta-cell enriched tissue obtained by laser capture microdissection from subjects with type 2 diabetes. *PLoS One* **5**, e11499 (2010).
80.Nishi K, *et al.* Branched-chain keto acids inhibit mitochondrial pyruvate carrier and suppress gluconeogenesis in hepatocytes. *Cell Rep* **42**, 112641 (2023).
81.Xiao W, *et al.* Branched-chain α-ketoacids aerobically activate HIF1α signalling in vascular cells. *Nat Metab* **6**, 2138-2156 (2024).
82.Wang TJ, *et al.* Metabolite profiles and the risk of developing diabetes. *Nature medicine* **17**, 448-453 (2011).
83.Biswas D, *et al.* Branched-chain ketoacid overload inhibits insulin action in the muscle. *J Biol Chem* **295**, 15597-15621 (2020).
84.Blair MC, *et al.* Branched-chain amino acid catabolism in muscle affects systemic BCAA levels but not insulin resistance. *Nat Metab* **5**, 589-606 (2023).
85.Karusheva Y, *et al.* Branched-Chain Amino Acids Associate Negatively With Postprandial Insulin Secretion in Recent-Onset Diabetes. *J Endocr Soc* **5**, bvab067 (2021).
86.Oresic M, *et al.* Dysregulation of lipid and amino acid metabolism precedes islet autoimmunity in children who later progress to type 1 diabetes. *J Exp Med* **205**, 2975-2984 (2008).
87.Funchal C, Gottfried C, De Almeida LM, Wajner M, Pessoa-Pureur R. Evidence that the branched-chain alpha-keto acids accumulating in maple syrup urine disease induce morphological alterations and death in cultured astrocytes from rat cerebral cortex. *Glia* **48**, 230-240 (2004).
88.Guo X, *et al.* BCKA down-regulates mTORC2-Akt signal and enhances apoptosis susceptibility in cardiomyocytes. *Biochemical and biophysical research communications* **480**, 106-113 (2016).
89.Lu G, *et al.* A novel mitochondrial matrix serine/threonine protein phosphatase regulates the mitochondria permeability transition pore and is essential for cellular survival and development. *Genes Dev* **21**, 784-796 (2007).
90.D'Addio F, *et al.* The IGFBP3/TMEM219 pathway regulates beta cell homeostasis. *Nat Commun* **13**, 684 (2022).
91.D'Addio F, *et al.* TMEM219 regulates the transcription factor expression and proliferation of beta cells. *Front Endocrinol (Lausanne)* **15**, 1306127 (2024).

92.Karusheva Y, *et al.* Short-term dietary reduction of branched-chain amino acids reduces meal-induced insulin secretion and modifies microbiome composition in type 2 diabetes: a randomized controlled crossover trial. *Am J Clin Nutr* **110**, 1098-1107 (2019).
93.2. Classification and Diagnosis of Diabetes: Standards of Medical Care in Diabetes-2019. *Diabetes Care* **42**, S13-s28 (2019).
94.Supriya R, *et al.* Adipokine Profiling in Adult Women With Central Obesity and Hypertension. *Front Physiol* **9**, 294 (2018).
95.Cheong LY, *et al.* Fibroblastic reticular cells in lymph node potentiate white adipose tissue beiging through neuro-immune crosstalk in male mice. *Nat Commun* **14**, 1213 (2023).
96.Lu G, Sun H, Korge P, Koehler CM, Weiss JN, Wang Y. Functional characterization of a mitochondrial Ser/Thr protein phosphatase in cell death regulation. *Methods Enzymol* **457**, 255-273 (2009).
97.Olson KC, Chen G, Lynch CJ. Quantification of branched-chain keto acids in tissue by ultra fast liquid chromatography–mass spectrometry. *Analytical biochemistry* **439**, 116-122 (2013).
98.Walvekar A, Rashida Z, Maddali H, Laxman S. A versatile LC-MS/MS approach for comprehensive, quantitative analysis of central metabolic pathways [version 1; referees: 2 approved]. *Wellcome open research* **3**, 122-122 (2018).
99.Yan M, *et al.* Metabolomics profiling of metformin-mediated metabolic reprogramming bypassing AMPKα. *Metabolism* **91**, 18-29 (2019).
100.Lomenick B, *et al.* Target identification using drug affinity responsive target stability (DARTS). *Proceedings of the National Academy of Sciences - PNAS* **106**, 21984-21989 (2009).

Acknowledgement

We would like to thank Dr. Xi Chen for her kind help in collecting serum and tissue samples in BCKA-fed mice. We thank the department of University Life Science in The Hong Kong Polytechnic University for providing instruments and instructions. This project was supported by National Natural Science Foundation of China (81970675 and 92357305), Hong Kong Research Grant Council (RGC) Collaborative Research Fund (C5044-23G) and General Research Fund (15101221), Shenzhen Municipal

Science and Technology Innovation Commission Basic Research General Programme: 20210324130202006 and PolyU internal funding (P0040979, P0036848 and P0059102) to Dr. Kenneth King-yip Cheng, AoE/M-707/18/RGC Area of Excellence to Dr. Aimin Xu and Department of Defense (W81XWH2010592) to Dr. Chen Cao.

Author contributions

H.L. and M.Y.H. conducted most of the experiments and drafted and revised the manuscript. Y.Y. and B.W. collected human samples and conducted data analysis. S.M. and A.M.M. performed some immunohistochemical experiments. W.W., P.S. and H.P helped with LC-MS/MS measurement for BCAA/BCKA and TCA cycle intermediates. A.X. provided LDHA floxed mice and revised the manuscript. S.Y. and J.C. supervised and conducted BCKA-LDHA docking site analysis. C.G provided PPM1K global KO mice, provided supervision on the animal study and reviewed the manuscript. P.M.S. collected human serum samples and clinical data in Hong Kong. X.L. provided pancreatic slides, islets, serum and clinical data from T2D humans. K.K.C. acquired the funding, provided resources, supervised the project and wrote the manuscript. K.K.C. and X.L jointly supervised this work. All authors reviewed and approved the final manuscript.

Competing interests

All the authors declare no competing interests.

Figure Legends/Captions (for main text figures)

Fig. 1: Aberrant BCAA catabolism in mouse and human islets in diabetic condition.

a-c, 20-week-old *db/db* mice and their lean littermates (*db/+)* were used. **a** Immunohistochemical staining was performed for BCAT2 (branched-chain amino acid transaminase 2), total BCKDH-A (branched-chain keto acid dehydrogenase E1), pBCKDH-A (phospho-BCKDH-A), PPM1K (protein phosphatase 1K), and BDK (branched-chain ketoacid dehydrogenase kinase) in pancreatic sections. The arrow indicates the location of the islet. Scale bars, 100 μm. **b** Quantification of IHC signals. n=7 mice and 5 mice for BCAT2 staining. n=7 mice per group for the other staining. **c** Intracellular levels of BCAA, BCKA, and C2/C3/C5-acylcarnitines in the isolated islets. n=8. **d** mRNA and protein expressions of BCAA metabolic enzymes in islets from non-T2D (ND) and type 2 diabetes (T2D) humans. Transcriptome (n=82 and 8) and proteome (n=118 and 15) datasets from HumanIslets online portal were used. **e-g** Immunofluorescence (IF) staining of PPM1K (red), total BCKDH-A (red) and pBCKDH-A (red), along with insulin (green) in pancreatic sections from ND and T2D human donors. The arrow indicates the location of the islet. Scale bars, 100 μm. **g** Quantification of IF signals. n=8. Data are presented as mean ± SEM. Statistical significance for **d** was determined using Benjamini-Hochberg adjusted p-values < 0.05 of student t-test. Other significances were calculated using a two-tailed independent Student's t-test. *$p < 0.05$ and **$p < 0.01$.

Fig. 2: Excessive BCKA impairs glucose-stimulated insulin secretion (GSIS) in human and murine pancreatic β-cells.

a-c Static insulin secretion in response to 2 mM (basal) and 20 mM glucose. **a** Islets isolated from male C57BL/6J mice and cultured with a BCKA mixture (equal concentrations of KIC, KMV and KIV). n=5 for basal and n=6 for glucose-stimulated groups. n represents the number of independent biological replicates (tubes), with each replicate containing a pool of 5 size-matched islets. **b** MIN6 cells were pre-treated with vehicle or BCKA (30 μM each of KIC, KMV and KIV) in the presence or absence of BT2 (10 μM) for 48 hours. n=4 per group, except for the basal BCKA+BT2 group (n=3). n represents the number of independent culture wells (biological replicates). **c** Human islets pre-treated with vehicle or BCKA (30 μM each of KIC, KMV and KIV) for 48 hours. n=5. **d-g,** INS-1E β-cells were transfected with siRNA against (**d-e**) *Bckdha*, (**f-g**) *Ppm1k*, or *scramble* for 24 hours, followed by culture in normal or BCAA-free medium for 24 hours. **d** Immunoblotting analysis and densitometric quantification of BCKDH-A. n=3. n represents the number of independent biological samples. **e** Static GSIS assay. n=8. **f** Immunoblotting analysis and densitometric quantification of PPM1K. n=4. n represents the number of independent biological samples. Representative blots are shown. **g** GSIS assay. n=4. **h**, Static GSIS in islets isolated from 12-week-old male global PPM1K KO mice and WT controls. n=8 (WT) and n=6 (KO) for the basal groups, and n=9 per group for the glucose-stimulated groups. n represents independent biological replicates, with each replicate containing 5 size-matched islets. Data are presented as mean ± SEM. Significance was determined using one-way ANOVA with Tukey correction for multiple comparisons in **a, b, e, g**, and a two-tailed independent Student's t-test for the remaining data.

Fig. 3: Chronic BCKA supplementation impairs GSIS and induce glucose intolerance in mice.

a-**g**, 16-week-old male C57BL/6J mice were given drinking water containing BCKAs (KIC, KMV, and KIV, each at 5 mg/mL), or a vehicle for 6 weeks. n=6 mice per group. **a** Circulating level of BCKA under fed conditions. **b** Insulin tolerance tests (ITT) were performed after 3 weeks of BCKA feeding. **c-f** Glucose tolerance tests (GTT) were conducted after (**c**) 2 weeks and (**e**) 6 weeks of BCKA feeding, with (**d, f**) corresponding fold changes in serum insulin during GTT. **g** Arginine-induced insulin secretion was assessed after 4 weeks of BCKA feeding. **h-i** Islets isolated from 12-week-old C57BL/6J mice were incubated with BCKAs (KIC, KMV, and KIV each at 30 μM) or vehicle for 48 hours. **h** Static insulin secretion stimulated by glucose (2 mM or 20 mM) or KCl (40 mM). n=5. **i** Dynamic GSIS assay. n=3. Individual p values for -6–0min (0.4315, 0.4176, 0.1633), 12–27 min (0.8863, 0.7631, 0.5497, 0.3000, 0.3522, 0.7980), 30–42 min (0.4800, 0.9781, 0.7814, 0.4983, 0.8876). Data are presented as mean ± SEM. Statistical significance was determined using a two-tailed independent Student's t-test.

Fig. 4: Pancreatic β-cell-specific deletion of PPM1K impairs GSIS and induces glucose intolerance in mice.

Male PPM1K β-KO mice and their WT littermates, fed a standard chow diet, were used in the study. **a** *Ppm1k* mRNA expression in pancreatic islets isolated from 10-week-old mice. n=4. **b** Intracellular BCKA levels in islets from 12-week-old mice. 100 size-matched islets per sample. **c-d** Glucose tolerance test (GTT) and fold change in serum insulin during GTT in 10-week-old mice. **e** Insulin tolerance test (ITT) in 12-week-old mice. **f** Arginine-induced insulin secretion in 21-week-old mice. **b-f** n=5 mice (WT) and n=6 mice (β-KO). **g** Static insulin secretion in islets isolated from 20-week-old WT and β-KO mice. Islets were stimulated with glucose or KCL as indicated. Basal, n=5 per group; Glucose, n=6 per group; KCL, n=4 for WT and n=5 for β-KO. **h** Dynamic GSIS assay in islets from 20-week-old WT and β-KO mice. n=3. Data are presented as mean ± SEM. Statistical significance was determined using a two-tailed independent Student's t-test.

Fig. 5: Chronic high BCKA dampens glucose flux into the TCA cycle by modulating pyruvate metabolism in pancreatic β-cells.

a Schematic of the GSIS triggering pathway. **b-e** MIN6 β-cells and **g-l** pancreatic islets from 12-week-old C57BL/6J mice were treated with vehicle or BCKA (30 μM each of KIC, KMV and KIV)) for 48 hours. **b** 2-deoxy-D-glucose (2-DG) uptake assay. n=7. **c** Relative glucose-stimulated ATP production. n=6 for the Glucose-Vehicle group and n=5 for all other groups. **d-e** Glycolytic stress test in MIN6 β-cells concomitantly treated with or without BT2 (10 μM) for 48 hours. (**d)** ECAR and (**e)** OCR in response to stimulations with glucose, oligomycin, and 2-DG. n=9. **d** Individual p value for Vehicle vs BCKA: 0–20 min (0.3071, 0.2243, 0.2628), 21–60 min (0.0014, 0.0009, 0.0008, 0.0004), 61–80 min (0.3808, 0.9834, 0.1106), 81–110 min (0.5186, 0.1672, 0.0734). Individual p value for BCKA vs BCKA + BT2: 0–20 min (0.1729, 0.0688, 0.0394), 21–60 min (0.0067, 0.0013, 0.0017, 0.0008, 0.9471), 61–80 min (0.1268, 0.7669, 0.2508), 81–110 min (0.1763, 0.1672, 0.1211). **e** Individual p value for Vehicle vs BCKA: 0–20

min (0.6808, 0.8920, 0.8473), 21–60 min (0.0046, 0.0030, 0.0023, 0.0020), 61–80 min (0.2134, 0.7288, 0.9864), 81–110 min (0.4238, 0.5092, 0.7873). Individual p value for BCKA vs BCKA + BT2: 0–20 min (0.9957, 0.9120, 0.9021), 21–60 min (0.0055, 0.0046, 0.0055, 0.0060), 61–80 min (0.5165, 0.9860, 0.8348), 81–110 min (0.5701, 0.7194, 0.8707). Vehicle vs BCKA, *$p < 0.05$ and **$p < 0.01$. BCKA vs BCKA + BT2, #$p < 0.05$ and ##$p < 0.01$. **f** Schematic showing the labeling pattern of [U-$^{13}C_6$] glucose metabolism into the first round of the TCA cycle. Orange and gray circles represent ^{13}C flux via PDH and PC, respectively. Black circles represent ^{12}C. **g-l**, $^{13}C_6$ glucose metabolic flux analysis. Pancreatic islets were incubated with 2 mM $^{13}C_6$ glucose for 30 minutes, followed by 30 minutes of labeling with $^{13}C_6$ glucose (20 mM). Fractional enrichments of $^{13}C_6$ glucose-derived lactate (**g**), pyruvate (**h**), citrate (**i**), α-KG (**j**), succinate (**k**), and malate (**l**). n=3 (300 size-matched islets per sample). Data are presented as mean ± SEM. Statistical significance was determined using one-way ANOVA with Tukey correction for multiple comparisons in **d** and **e**, and two-tailed independent Student's t-test for the remaining data.

Fig. 6: Inhibition of LDHA abrogates the suppressive effect of BCKA on GSIS in mice.

a Immunoblotting analysis and quantification of LDHA in MIN6 cells treated with vehicle or BCKA (30 μM each of KIC, KMV and KIV). n=5 for Vehicle and n=6 for BCKA. Representative blots are shown. **b-c** LDHA enzymatic activity in (**b**) mouse islets treated with BCKA (30 μM) for 48 hours, and in (**c**) MIN6 cell lysates incubated with BCKA (30 μM) at 4°C for 3 hours. n=3. **d** Ratio of M+3 lactate to M+3 pyruvate in human islets stimulated with $^{13}C_6$ glucose (10 mM) for 30 minutes. n=4. **e** 50 ng of purified recombinant human LDHA were incubated with vehicle or BCKA (30 μM) at 4°C for 12 hours (pH 7.4). Enzymatic activity was analyzed by lactate conversion after the addition of substrates. n=3. **f-k** Male LDHA β-KO mice and WT littermates were fed BCKA (5 mg/mL each of KIC, KMV, and KIV in drinking) or vehicle for 6 weeks. n=4 mice per group. **f** Immunofluorescence staining of LDHA (red) and insulin (green) in isolated islets. The arrow indicates the location of the islet. Scale bars: 100 μm. **g-h** GTT after 5 weeks of BCKA feeding and AUC. **i-j** Fold change in glucose-stimulated serum insulin and AUC. **k** ITT after 6 weeks of BCKA feeding. **l** Static GSIS in isolated WT and LDHA β-KO islets treated with BCKA or vehicle for 48 hours. n=5. **g-i** Individual p values are shown in red for WT+Vehicle vs WT+BCKA, and in yellow for WT+BCKA vs LDHA β-KO+BCKA. Data are presented as mean ± SEM. Statistical significance was determined using a two-tailed independent Student's t-test for **a-e**, and one-way ANOVA with Tukey correction for multiple comparisons for the remaining data.

Fig. 7: BCKA promotes LDHA dimerization and its enzymatic activity.

a 3D diagram of the binding modes between human dimeric LDHA (PDB: 8FW6) and KIC, KMV, and KIV. The binding free energy of each molecule is shown. Chain A is colored orange; Chain B is magenta; KIC, KMV, and KIV are represented as green stick models; hydrogen bonds are indicated by blue dashed lines. **b** Representative surface plasmon resonance (SPR) assay showing the binding interactions between human recombinant LDHA protein and KIC, KMV, KIV and pyruvate (Pyr). Sensorgrams illustrate the

binding and dissociation phases, with equilibrium dissociation constant (K_D) values calculated to assess binding strength. **c** Protein crosslinking assay for tetrameric, dimeric, and monomeric forms of LDHA in whole-cell lysates of mouse islets (470 size-matched islets per sample) and INS-1E cells incubated with vehicle or BCKA (30 μM each of KIC, KMV and KIV) for 48 hours. Glutaraldehyde was added to the cell lysate as a crosslinking agent to stabilize protein interactions. **d** Effect of BCKA on the dimerization and tetramerization of recombinant human LDHA protein. Monomeric LDHA control was prepared by heating at 99°C for 5 minutes. **e** 293T cells were transfected with empty vector, or plasmids overexpressing LDHA WT or Ser210A (1MUT), Ser202A/Ser210A/Thr307A (3 MUT) or Gly 203A/Gly208A/Asn205A/Ser 210A (4 MUT). The cell lysates were incubated with 0, 0.2 mM or 2 mM BCKA, followed by DARTS analysis of proteinase K (PK)-mediated LDHA degradation. Protein abundance in total cell lysates (TCL) was visualized using silver staining. **c-e** Each experiment was independently repeated at least three times with similar results.

Fig. 8: BCKA impairs glucose-stimulated insulin secretion by redirection of glucose metabolism to the LDHA-lactate axis.

Under healthy conditions, glucose is metabolized through glycolysis and the mitochondrial TCA cycle to generate coupling factors like ATP, which are essential for first-phase insulin secretion. BCAA-derived BCKAs are catabolized in mitochondria via the BCKDH complex, activated by PPM1K and deactivated by BDK through dephosphorylation of BCKDH-A.

In diabetes, disrupted PPM1K-BCKD-A signal axis in pancreatic β-cells or chronic elevation of circulating BCKA and BCAA leads to BCKA accumulation in the cells. BCKA promotes the conversion of LDHA from its inactive monomeric form to its active dimeric form. Activated LDHA rewires glucose metabolism to lactate production, which limits pyruvate entry into the TCA cycle, reduces ATP generation, and impairs insulin secretion, thereby contributing to pathogenesis of type 2 diabetes. Cell membrane and insulin icons: Created in BioRender. Lin, Z. (2026) https://BioRender.com/37y39de.

Editorial summary:

This study reveals that BCAA-derived BCKAs impair glucose-induced insulin secretion via activation of LDHA, a disallowed enzyme in pancreatic β-cells. Blocking this signalling axis restores insulin secretion, offering a new target against diabetes

Peer review information: *Nature Communications* thanks Gang Bai, and the other, anonymous, reviewer(s) for their contribution to the peer review of this work. A peer review file is available.

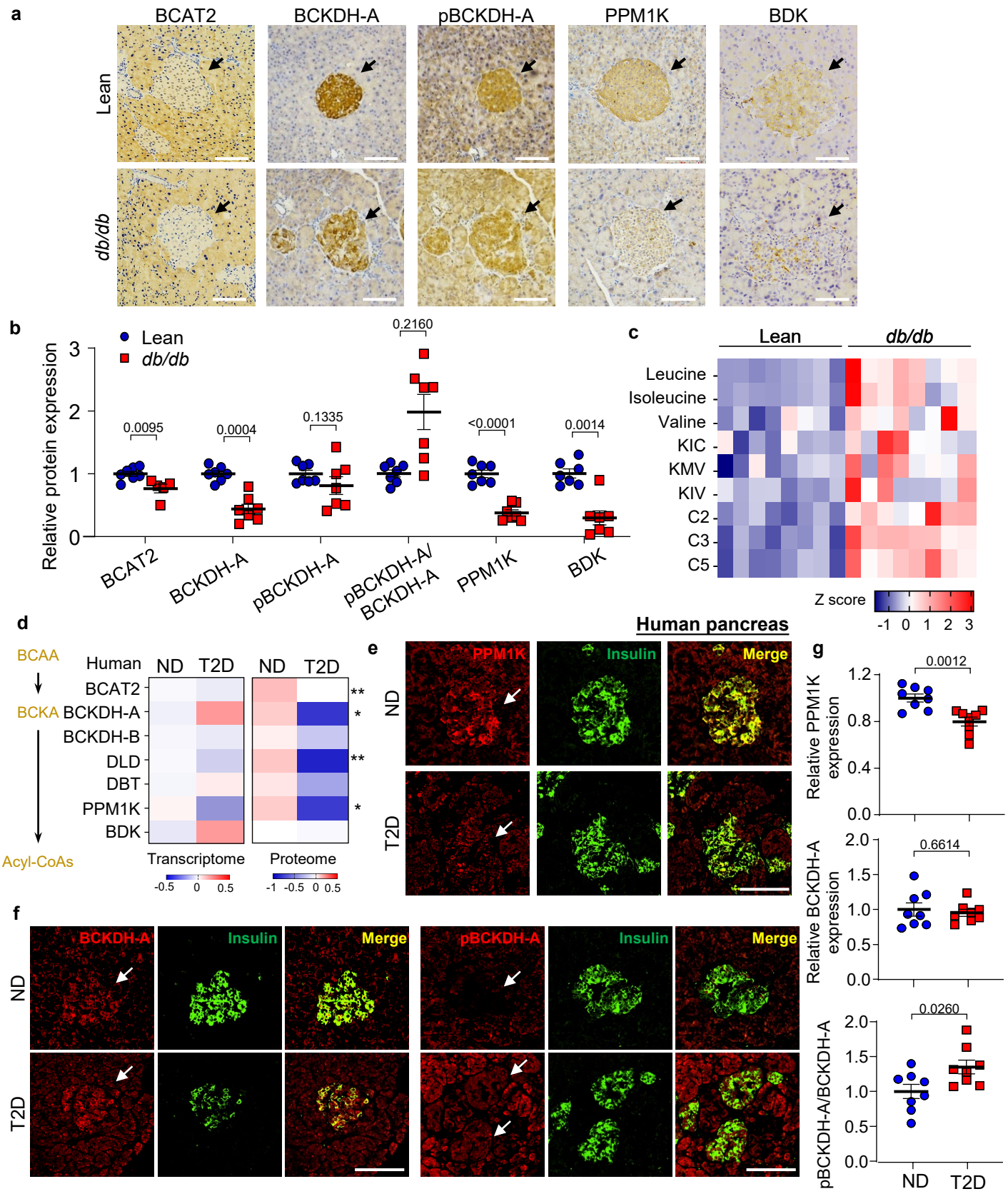
a
BCAT2
BCKDH-A
pBCKDH-A
PPM1K
BDK
Lean
db/db
b
Lean
db/db
Relative protein expression
0.0095
0.0004
0.1335
0.2160
<0.0001
0.0014
BCAT2
BCKDH-A
pBCKDH-A
pBCKDH-A/ BCKDH-A
PPM1K
BDK
c
Lean
db/db
Leucine
Isoleucine
Valine
KIC
KMV
KIV
C2
C3
C5
Z score
d
BCAA
BCKA
Acyl-CoAs
Human
ND
T2D
BCAT2
BCKDH-A
BCKDH-B
DLD
DBT
PPM1K
BDK
Transcriptome
Proteome
e
Human pancreas
PPM1K
Insulin
Merge
ND
T2D
g
Relative PPM1K expression
0.0012
Relative BCKDH-A expression
0.6614
pBCKDH-A/BCKDH-A
0.0260
ND
T2D
f
BCKDH-A
Insulin
Merge
pBCKDH-A
Insulin
Merge
ND
T2D

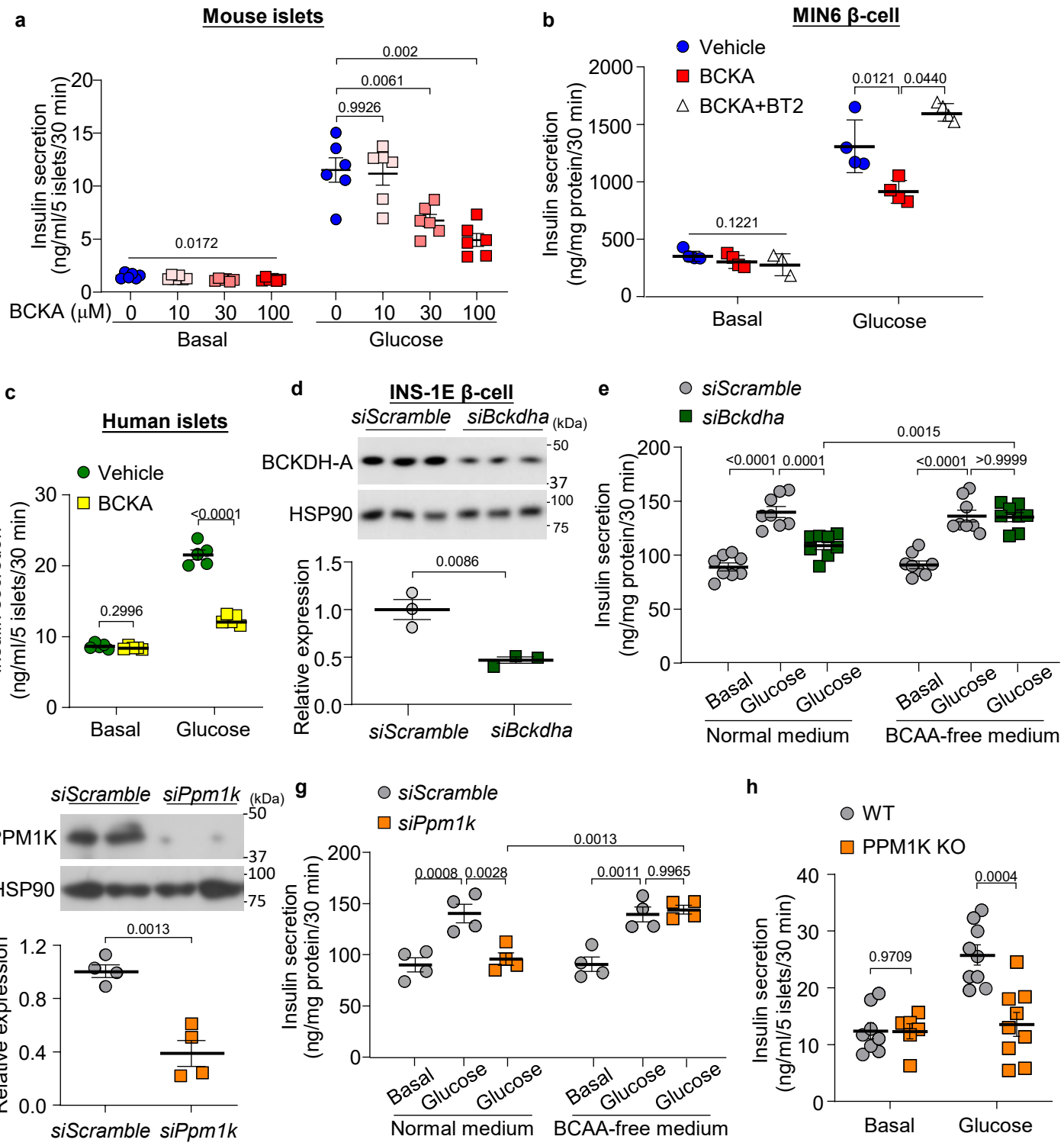
a
Mouse islets
Insulin secretion (ng/ml/5 islets/30 min)
BCKA (μM) 0 10 30 100 0 10 30 100
Basal
Glucose
0.0172
0.9926
0.0061
0.002
b
MIN6 β-cell
Vehicle
BCKA
BCKA+BT2
Insulin secretion (ng/mg protein/30 min)
0.1221
0.0121
0.0440
Basal
Glucose
c
Human islets
Vehicle
BCKA
Insulin secretion (ng/ml/5 islets/30 min)
0.2996
<0.0001
Basal
Glucose
d
INS-1E β-cell
siScramble
siBckdha
(kDa)
BCKDH-A
HSP90
50
37
100
75
Relative expression
0.0086
siScramble
siBckdha
e
siScramble
siBckdha
Insulin secretion (ng/mg protein/30 min)
<0.0001
0.0001
0.0015
<0.0001
>0.9999
Basal
Glucose
Glucose
Basal
Glucose
Glucose
Normal medium
BCAA-free medium
f
siScramble
siPpm1k
(kDa)
PPM1K
HSP90
50
37
100
75
Relative expression
0.0013
siScramble
siPpm1k
g
siScramble
siPpm1k
Insulin secretion (ng/mg protein/30 min)
0.0008
0.0028
0.0013
0.0011
0.9965
Basal
Glucose
Glucose
Basal
Glucose
Glucose
Normal medium
BCAA-free medium
h
WT
PPM1K KO
Insulin secretion (ng/ml/5 islets/30 min)
0.9709
0.0004
Basal
Glucose

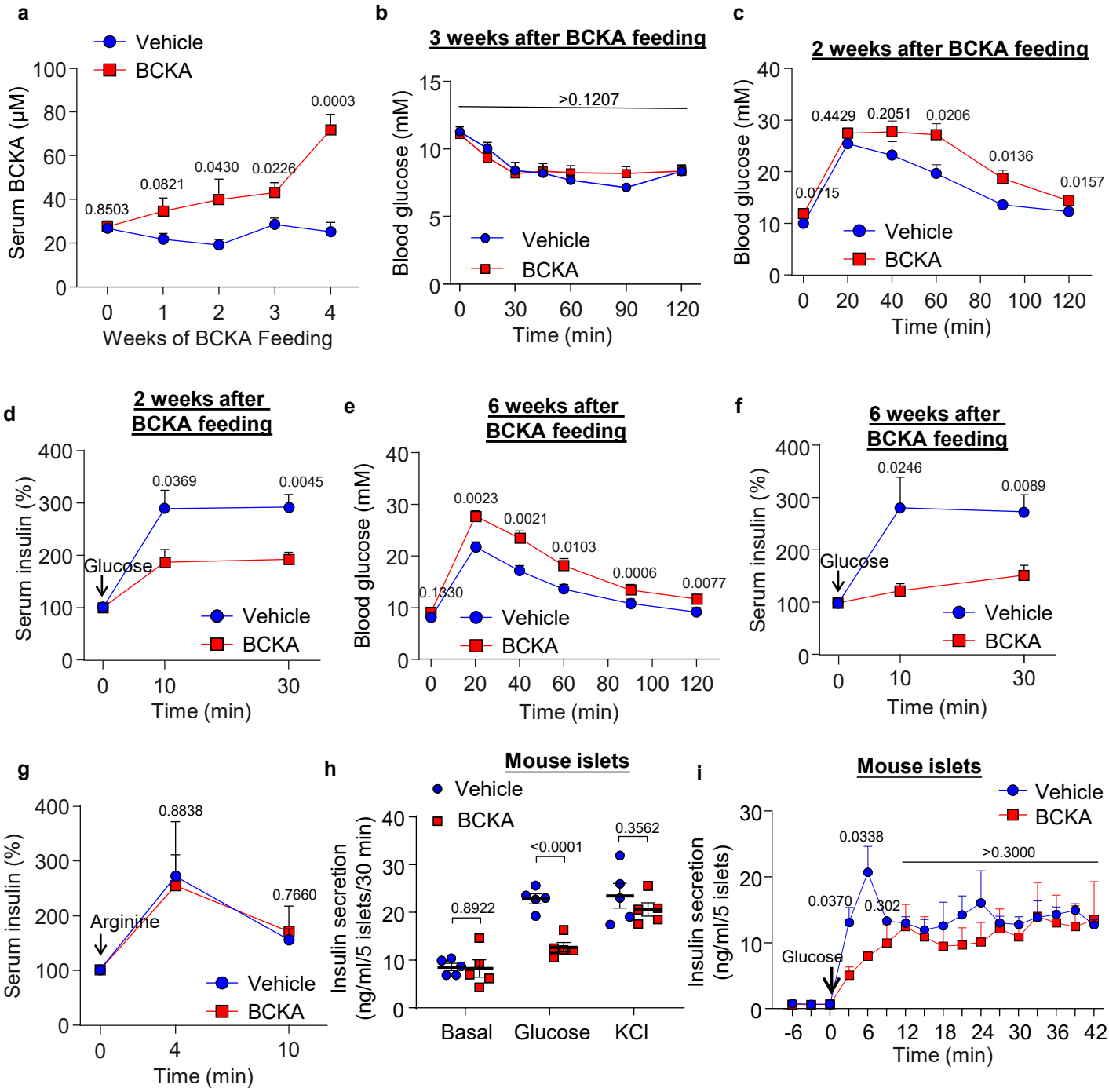
a
Vehicle
BCKA
Serum BCKA (μM)
0.8503
0.0821
0.0430
0.0226
0.0003
Weeks of BCKA Feeding
b
3 weeks after BCKA feeding
Blood glucose (mM)
>0.1207
Vehicle
BCKA
Time (min)
c
2 weeks after BCKA feeding
Blood glucose (mM)
0.0715
0.4429
0.2051
0.0206
0.0136
0.0157
Vehicle
BCKA
Time (min)
d
2 weeks after BCKA feeding
Serum insulin (%)
Glucose
0.0369
0.0045
Vehicle
BCKA
Time (min)
e
6 weeks after BCKA feeding
Blood glucose (mM)
0.1330
0.0023
0.0021
0.0103
0.0006
0.0077
Vehicle
BCKA
Time (min)
f
6 weeks after BCKA feeding
Serum insulin (%)
Glucose
0.0246
0.0089
Vehicle
BCKA
Time (min)
g
Serum insulin (%)
Arginine
0.8838
0.7660
Vehicle
BCKA
Time (min)
h
Mouse islets
Vehicle
BCKA
Insulin secretion (ng/ml/5 islets/30 min)
0.8922
<0.0001
0.3562
Basal
Glucose
KCl
i
Mouse islets
Vehicle
BCKA
Insulin secretion (ng/ml/5 islets)
0.0338
>0.3000
0.0370
0.302
Glucose
Time (min)

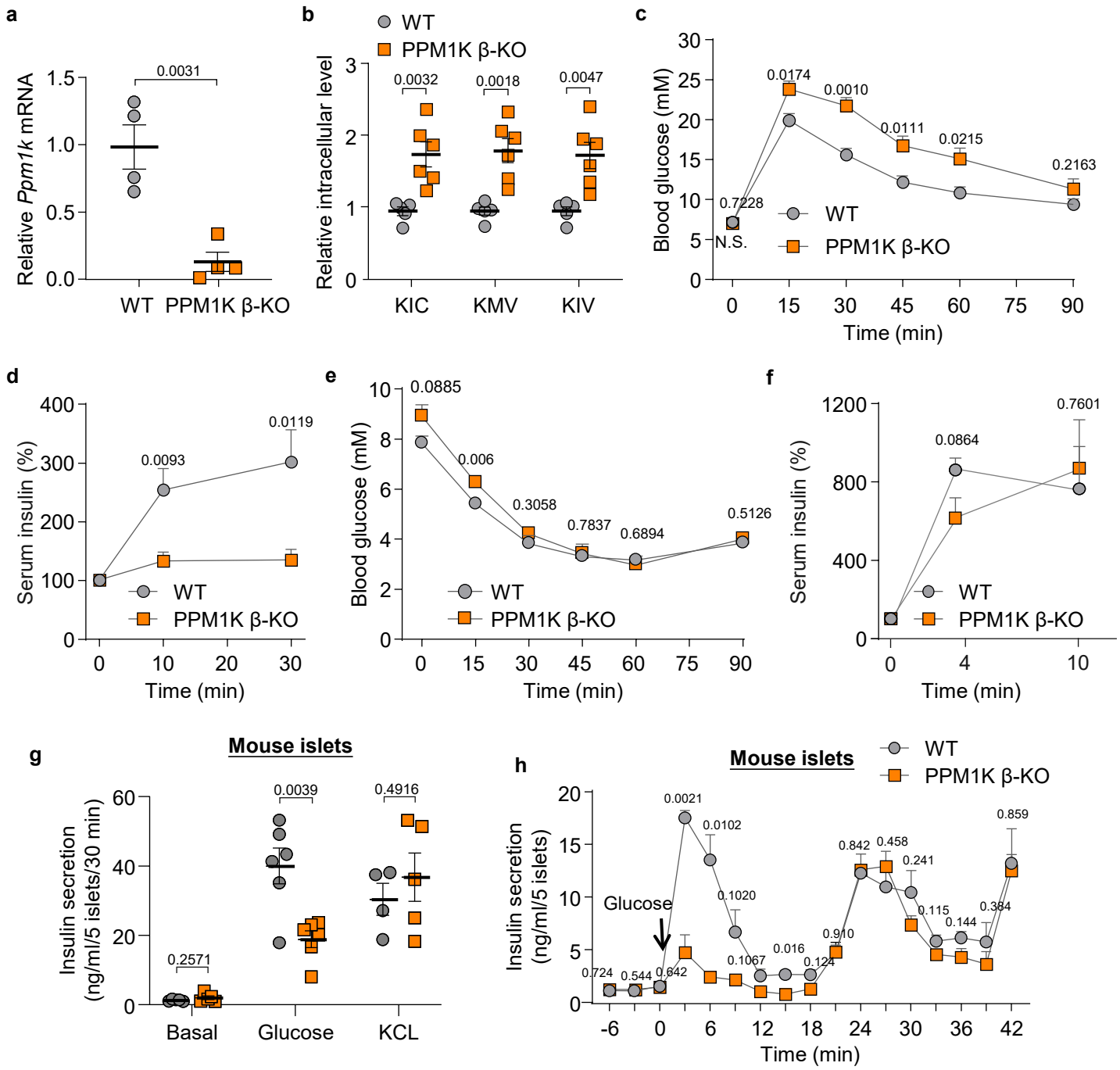
a
Relative Ppm1k mRNA
0.0031
WT
PPM1K β-KO
b
WT
PPM1K β-KO
Relative intracellular level
0.0032
0.0018
0.0047
KIC
KMV
KIV
c
Blood glucose (mM)
0.7228
N.S.
0.0174
0.0010
0.0111
0.0215
0.2163
WT
PPM1K β-KO
Time (min)
d
Serum insulin (%)
0.0093
0.0119
WT
PPM1K β-KO
Time (min)
e
Blood glucose (mM)
0.0885
0.006
0.3058
0.7837
0.6894
0.5126
WT
PPM1K β-KO
Time (min)
f
Serum insulin (%)
0.0864
0.7601
WT
PPM1K β-KO
Time (min)
g
Mouse islets
Insulin secretion (ng/ml/5 islets/30 min)
0.2571
0.0039
0.4916
Basal
Glucose
KCL
h
Mouse islets
WT
PPM1K β-KO
Insulin secretion (ng/ml/5 islets)
Glucose
0.0021
0.0102
0.1020
0.1067
0.016
0.124
0.910
0.842
0.458
0.241
0.115
0.144
0.384
0.859
0.724
0.544
0.642
Time (min)

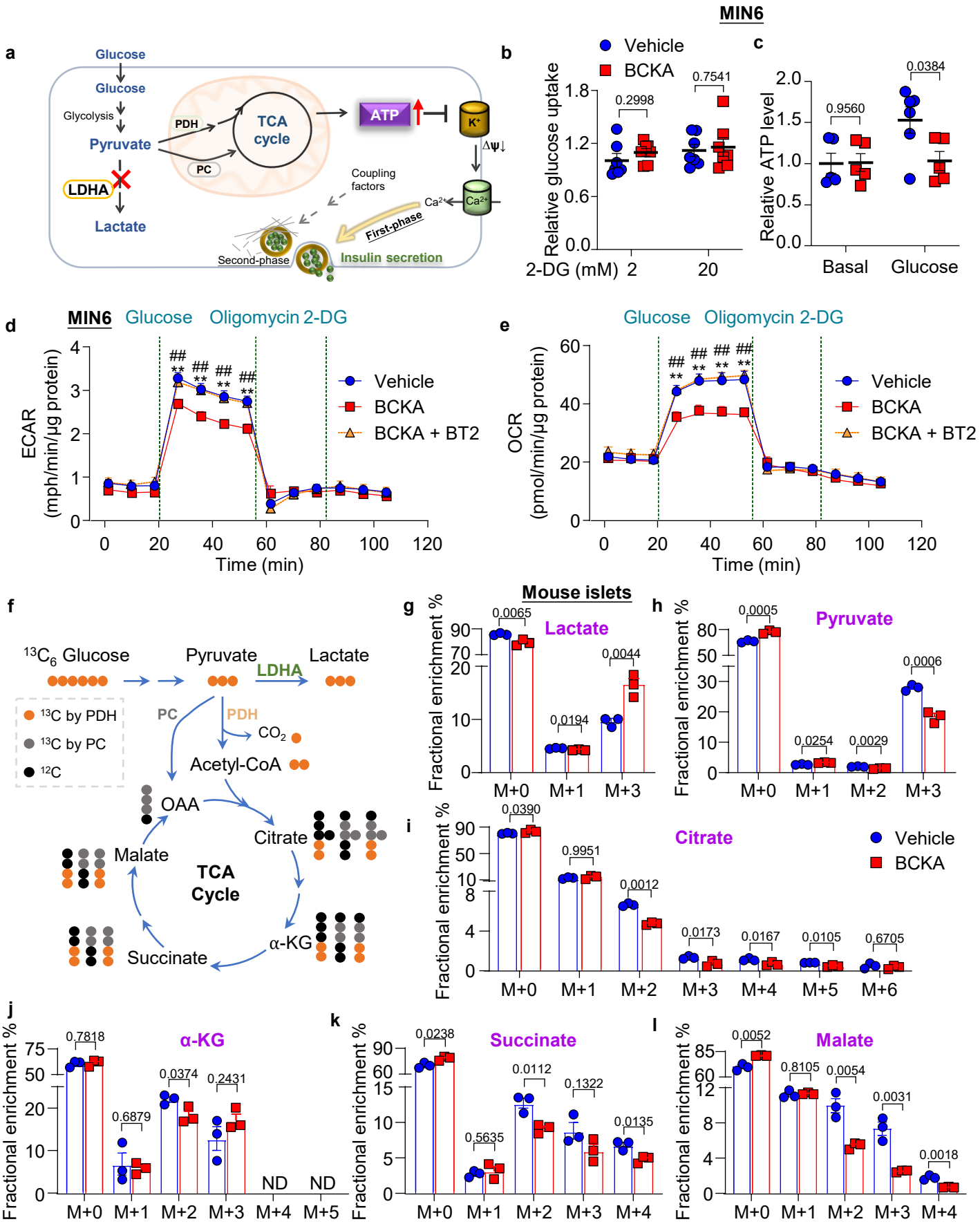
a
Glucose
Glucose
Glycolysis
Pyruvate
LDHA
Lactate
PDH
PC
TCA cycle
ATP
K+
ΔΨ↓
Coupling factors
Ca2+
Ca2+
First-phase
Second-phase
Insulin secretion
b
MIN6
Vehicle
BCKA
Relative glucose uptake
0.2998
0.7541
2-DG (mM) 2
20
c
Relative ATP level
0.9560
0.0384
Basal
Glucose
d
MIN6 Glucose Oligomycin 2-DG
ECAR (mph/min/μg protein)
Vehicle
BCKA
BCKA + BT2
Time (min)
e
Glucose Oligomycin 2-DG
OCR (pmol/min/μg protein)
Vehicle
BCKA
BCKA + BT2
Time (min)
f
13C6 Glucose
Pyruvate
Lactate
LDHA
13C by PDH
13C by PC
12C
PC
PDH
CO2
Acetyl-CoA
OAA
Citrate
Malate
TCA Cycle
α-KG
Succinate
Mouse islets
g
Lactate
Fractional enrichment %
0.0065
0.0194
0.0044
M+0
M+1
M+3
h
Pyruvate
0.0005
0.0254
0.0029
0.0006
M+0
M+1
M+2
M+3
i
Citrate
Vehicle
BCKA
0.0390
0.9951
0.0012
0.0173
0.0167
0.0105
0.6705
M+0
M+1
M+2
M+3
M+4
M+5
M+6
j
α-KG
0.7818
0.6879
0.0374
0.2431
ND
ND
M+0
M+1
M+2
M+3
M+4
M+5
k
Succinate
0.0238
0.5635
0.0112
0.1322
0.0135
M+0
M+1
M+2
M+3
M+4
l
Malate
0.0052
0.8105
0.0054
0.0031
0.0018
M+0
M+1
M+2
M+3
M+4

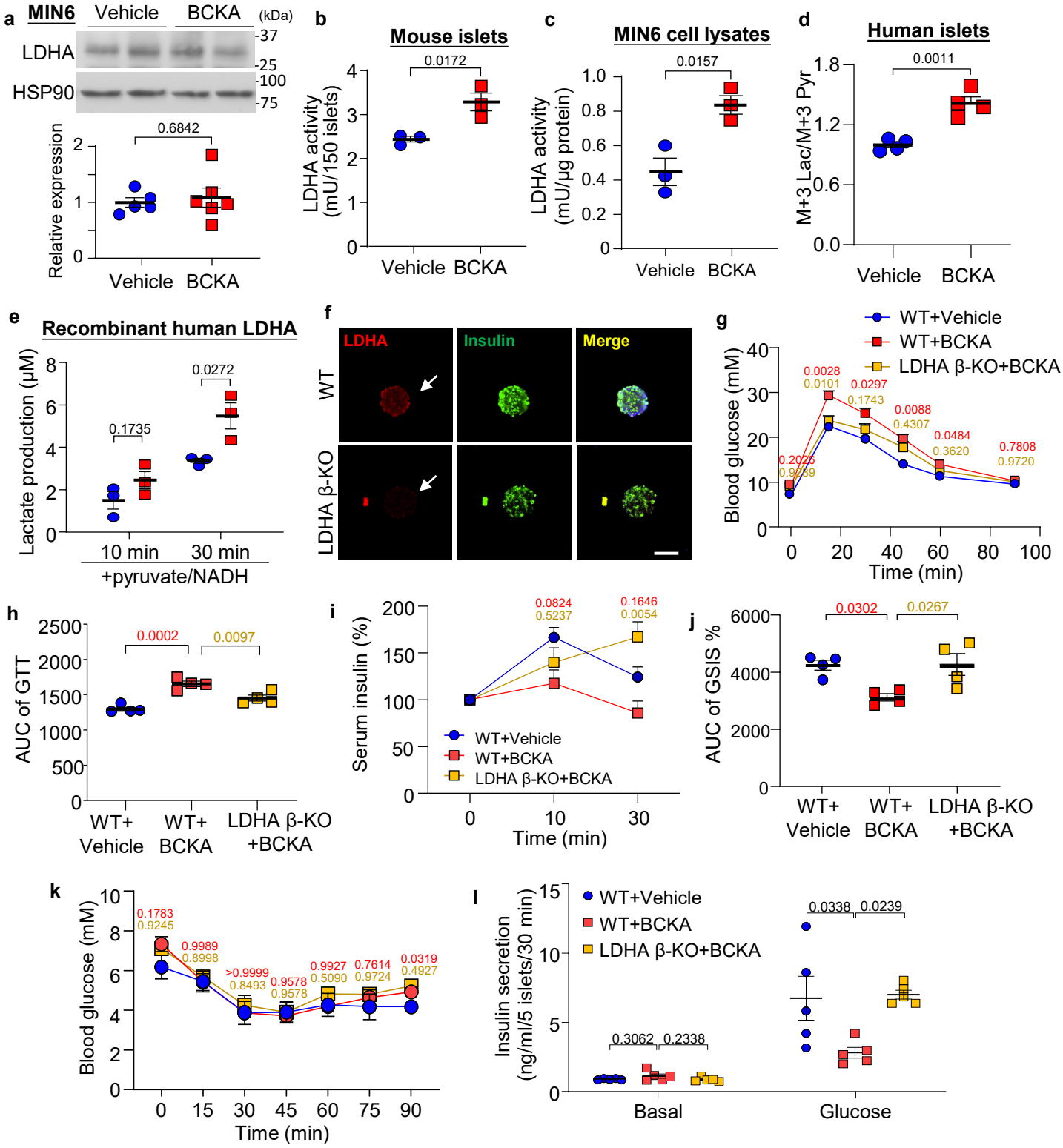
a
MIN6
Vehicle
BCKA
(kDa)
LDHA
HSP90
37
25
100
75
Relative expression
0.6842
Vehicle
BCKA
b
Mouse islets
0.0172
LDHA activity (mU/150 islets)
c
MIN6 cell lysates
0.0157
LDHA activity (mU/µg protein)
d
Human islets
0.0011
M+3 Lac/M+3 Pyr
e
Recombinant human LDHA
Lactate production (µM)
0.1735
0.0272
10 min
30 min
+pyruvate/NADH
f
LDHA
Insulin
Merge
WT
LDHA β-KO
g
WT+Vehicle
WT+BCKA
LDHA β-KO+BCKA
Blood glucose (mM)
Time (min)
h
AUC of GTT
0.0002
0.0097
WT+ Vehicle
WT+ BCKA
LDHA β-KO +BCKA
i
Serum insulin (%)
0.0824
0.5237
0.1646
0.0054
WT+Vehicle
WT+BCKA
LDHA β-KO+BCKA
Time (min)
j
AUC of GSIS %
0.0302
0.0267
WT+ Vehicle
WT+ BCKA
LDHA β-KO +BCKA
k
Blood glucose (mM)
0.1783
0.9245
0.9989
0.8998
>0.9999
0.8493
0.9578
0.9578
0.9927
0.5090
0.7614
0.9724
0.0319
0.4927
Time (min)
l
Insulin secretion (ng/ml/5 islets/30 min)
WT+Vehicle
WT+BCKA
LDHA β-KO+BCKA
0.0338
0.0239
0.3062
0.2338
Basal
Glucose

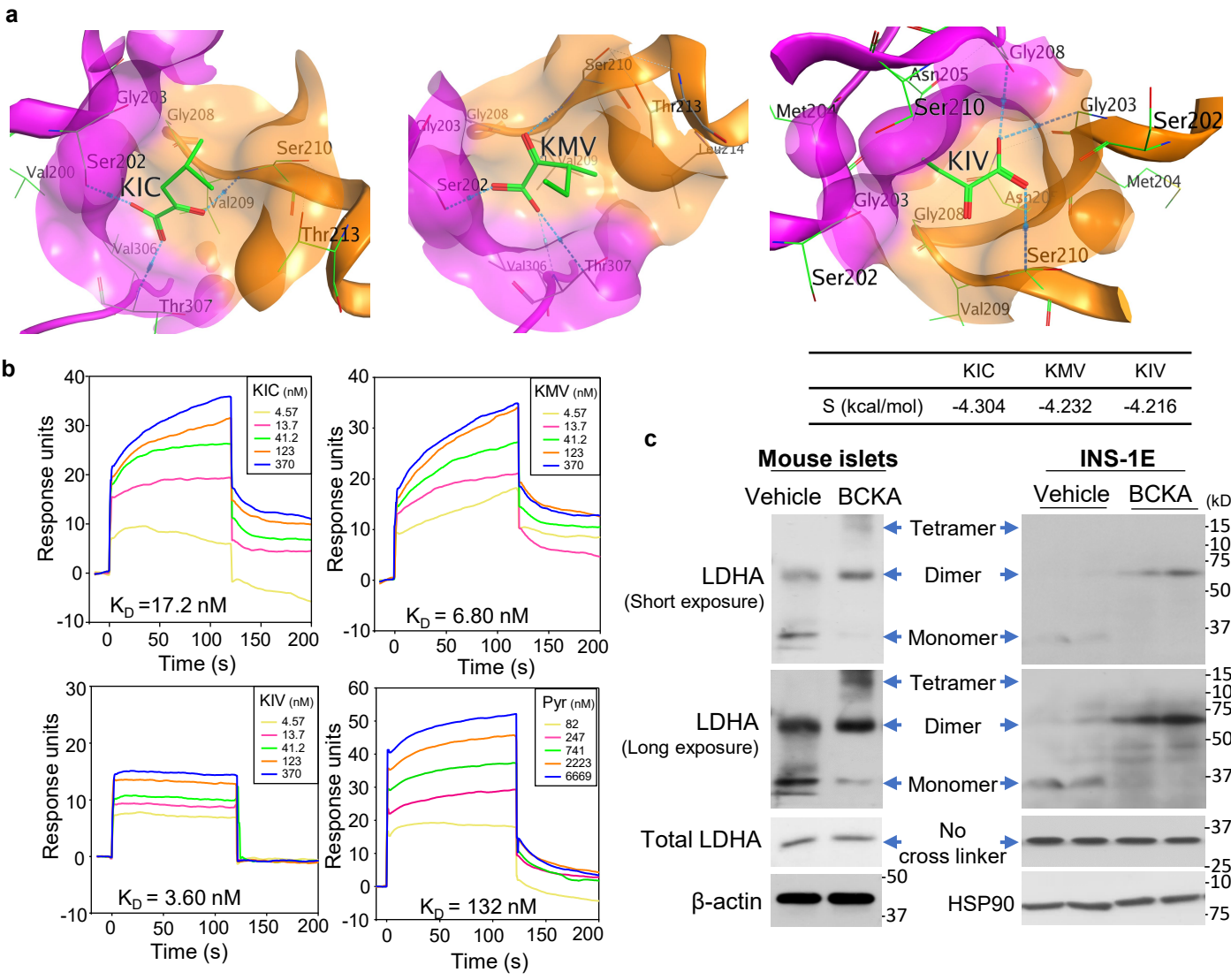

	KIC	KMV	KIV
S (kcal/mol)	-4.304	-4.232	-4.216

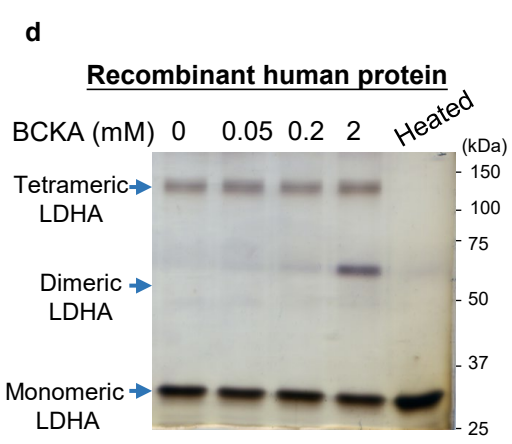

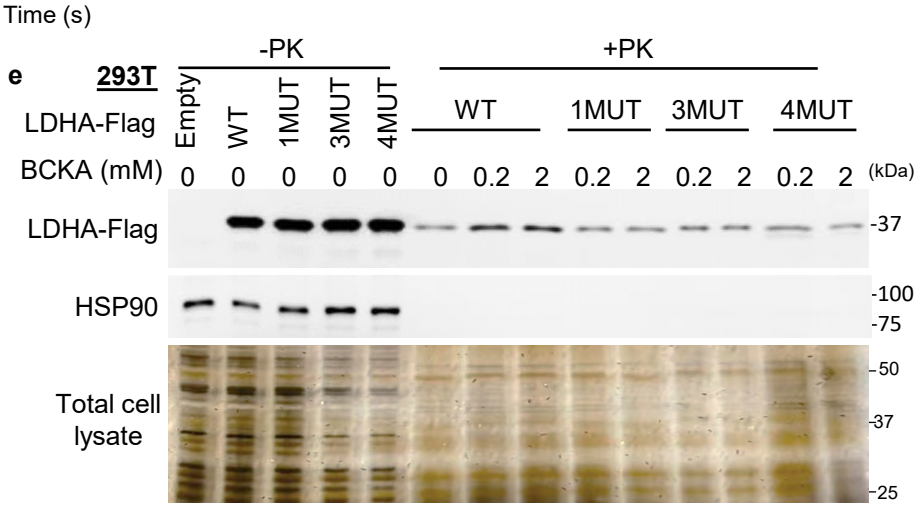

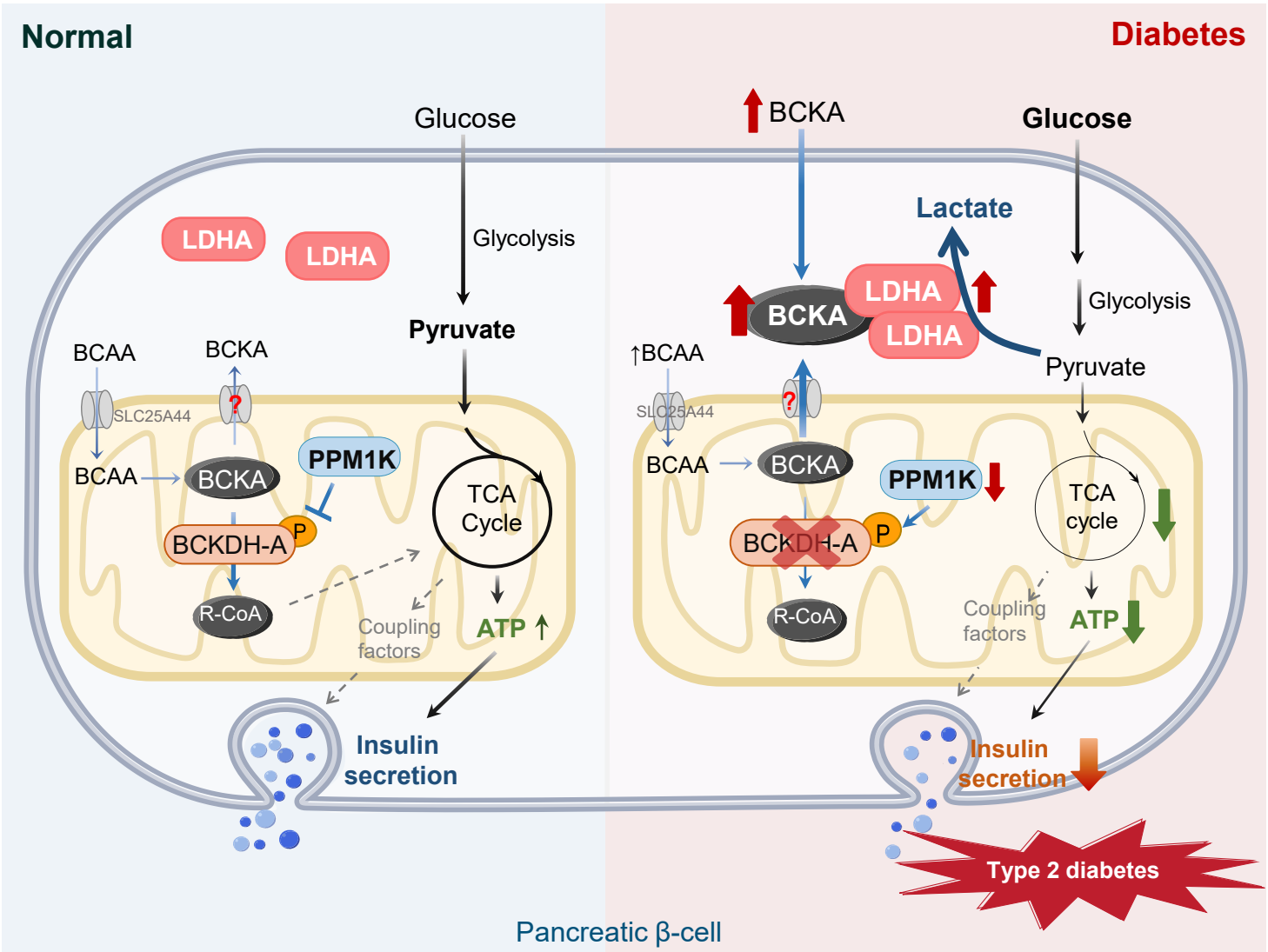
Normal
Diabetes
Glucose
LDHA
LDHA
Glycolysis
Pyruvate
BCAA
BCKA
SLC25A44
BCAA
BCKA
PPM1K
BCKDH-A
P
R-CoA
TCA Cycle
Coupling factors
ATP
Insulin secretion
BCKA
Glucose
Lactate
LDHA
LDHA
BCKA
Glycolysis
↑BCAA
Pyruvate
SLC25A44
BCAA
BCKA
PPM1K
TCA cycle
BCKDH-A
P
R-CoA
Coupling factors
ATP
Insulin secretion
Type 2 diabetes
Pancreatic β-cell